NASA CONTRACTOR REPORT 159175

"Pressure Modulator Radiometer (PMR) Tests"

E.L.G. ODELL

SPACE SCIENCES LABORATORY
GENERAL ELECTRIC COMPANY, SPACE DIVISION
P.O. Box 8555, Philadelphia, PA 19101

Contract NAS1-15044
SEPTEMBER 25, 1979

National Aeronautics and
Space Administration

Langley Research Center
Hampton, Virginia 23665
AC 804 827-3966

NASA CONTRACTOR REPORT 159175

"Pressure Modulator Radiometer (PMR) Tests"

E.L.G. ODELL

SPACE SCIENCES LABORATORY
GENERAL ELECTRIC COMPANY, SPACE DIVISION
P.O. Box 8555, Philadelphia, PA 19101

Contract NAS1-15044
SEPTEMBER 25, 1979

National Aeronautics and
Space Administration

Langley Research Center
Hampton, Virginia 23665
AC 804 827-3966

FOREWORD

This document constitutes the General Electric Company's Space Sciences Laboratory final technical report for the PMR Tests program.

The General Electric employees who contributed to the work described in the report are:

Tasks I and II - F. M. Cosmi, A. E. Kreft, E. L. G. Odell and G. W. Racette

Tasks III to VI - T. J. Maresca, E. L. G. Odell, F. O. Pancoast, G. W. Racette, D. J. Rutecki and W. C. Yager

The Technical Monitor for this contract was Mr. Dwayne E. Hinton.

APPROVED: E L G. Odell.
Program Manager

APPROVED: Carl S Anderson
Manager, Applied Physics

TABLE OF CONTENTS

LIST OF ILLUSTRATIONS

LIST OF ILLUSTRATIONS (continued)

1.0 PROGRAM SUMMARY

1.1 INTRODUCTION

This report documents the activities performed during the Pressure Modulator Radiometer (PMR) Tests program from its initiation on 4 August 1977 through 25 June 1979. The program was divided into two parts; the first was confined to an experimental set up that was built from available GE components and a 110 cm sample cell originally used on the COPE-CIMATS program. With this equipment it was only possible to examine the pressure modulator output signals resulting from a range of gas concentrations in the sample cell.

For the second part of the program, a 20 cm sample cell was modified so that trace gas properties in the atmosphere could be simulated in the laboratory. These gas properties were measured using an optical set up that was assembled specially for this task; it was similar to one section of the MAPS optical measurement system.

The PMR is an infrared sensor that was designed for measuring the radiation emitted by gases in the atmosphere. It was first used on a satellite to measure the temperature over several altitude ranges in the stratosphere using radiation emitted by carbon dioxide gas. Later it was used to measure carbon dioxide and other trace gases in the stratosphere and mesosphere. The other gases were water vapor, carbon monoxide, nitrous oxide, nitric oxide, and methane.

The PMR operates by using a novel form of non-dispersive gas correlation filter (NDGCF). In NDGCF instruments a sample of the species of gas that is being detected is contained in the instrument. In the PMR this gas is subjected to a cyclical change of pressure: the pressure cycle causes the optical characteristics of the gas to change in synchronism. This technique has the advantage over similar techniques in that it is an in-line optical system; as a result it does not suffer from imbalance difficulties experienced by other techniques.

The objective of the PMR tests program was to evaluate the pressure modulator technique for monitoring pollutant gases in the earth's atmosphere at altitude levels corresponding to the mid and lower troposphere. The pollutant gas to be used was CO and $C^{13}O_2$ and N_2O gases were to be used in the experiments as in situ temperature monitors. A pressure modulator cell had been loaned to General Electric by Prof. Houghton (University of Oxford, England), and it was used in both parts of the program.

The program started in August 1977 with the objective of determining the sensitivity of the PMR to fluctuations in background radiance and to changes in concentration of CO in a sample cell. In September 1978 the program was modified to improve the instrumentation and include a second pressure modulator.

As a result of funding redirections at the Langley Research Center (LaRC), there was a further modification in May 1979 that reduced the scope and direction of the program. A second modulator was not purchased and N_2O gas would be used as the in situ gas for temperature monitoring.

Section 1.2 gives a brief summary of the role of the instrument, Section 1.3 summarizes the results of Tasks 1 and 2, and Sections 1.4 to 1.6 summarizes the modified instrumentation and the results obtained with it. Section 2 describes Tasks 1 and 2 in more detail, Section 3 describes the design and development of the current equipment, and Sections 4, 5 and 6 give the results of the measurements; conclusions and recommendations are given in Section 7.

1.2 BACKGROUND

The upwelling radiation from a gas in the atmosphere several kilometers above ground level is very small in comparison with that of the earth's surface in most parts of the infrared spectrum. The radiance from the gas is a function of the gas concentration and the gas temperature. In most gas correlation filter

techniques there is no means of measuring the in situ gas temperature with the instrument making concentration measurements.

The pressure modulator technique does not have this difficulty and it is possible by using two pressure modulators in series, each containing a different gas and modulating them at different frequencies, to simultaneously measure the temperature and concentration of a gas in the atmosphere. The second gas used was one that is also a trace constituent of the atmosphere but one whose concentration is stable and well known; it is assumed that it is in local thermodynamic equilibrium with the gas whose concentration is to be determined.

Two possible problems must be addressed in applying the PM technique. The first is that random time varying fluctuations (twinkle) at the PM frequency may cause errors of measurement. Secondly the altitude range over which the sensor is most sensitive must be the same for both gases.

The prime objectives of this program are addressed to simulate the conditions that give rise to these problems by controlled laboratory experiments.

1.3 SUMMARY OF RESULTS FOR TASKS 1 AND 2

1.3.1 Background Modulation

The upwelling radiation from the earth's surface and atmosphere consists of a background continuum, superimposed on which is a complex structure of absorption and emission lines due to the gaseous atmospheric constituents. The regions between the spectra of the atmospheric gases exhibit a significant amount of spatial variation. A downward looking satellite sensor that scans the earth surface detects these radiance changes and records them as signals that vary as a function of time. For the PMR these signals could interfere with those signals emanating from the atmospheric gas which is being monitored, provided specific phase and amplitude requirements are met.

To properly simulate these signals in the laboratory, specially designed apparatus would have to be designed and used. Such experiments were not within the scope of Part I of this program but an attempt was made to estimate, with existing equipment, the effect of background modulation signals on a steady PM signal.

The background earth radiance was simulated by using a black body (BB) source. The spectra of carbon monoxide (CO) gas in the atmosphere was represented by CO in the 110 cm cell; the PM cell also contained CO. The black body radiance was modulated by rotating a blackened chopper wheel in front of the BB aperture. The frequency of rotation of the chopper was increased from about 1 Hz to a frequency exceeding that of the Pressure Modulator.

The output signals from the detector were recorded on magnetic tape and sent to LaRC for Fourier Analysis. The results of the analysis were that the percentage modulation of the background source were too high; the harmonics at the PMC frequency swamped the signals of the Pressure Modulator. Much lower (1-2%) modulation ratios would be needed to yield meaningful results.

1.3.2 Gas Concentration and Temperature Measurements

A 110 cm sample cell was used to contain $CO\text{-}N_2$, $C^{13}O_2\text{-}N_2$ and $CO\text{-}C^{13}O_2$ gas mixtures. A black body radiator was used to simulate the radiance from the earth's background. The measurements showed that the pressure modulator signal was a function of CO concentration and temperature. The measurements with $C^{13}O_2$ in the sample cell and CO in the PM cell indicated that there was either overlapping lines of the $C^{13}O_2$ and CO spectra or there was residual CO gas in the sample cell.

An unexpected feature of these experiments was exhibited by the nature of the change of the PM signal as the temperature of the gas in the sample cell was

increased above ambient temperature. An increase of PM signal was expected as the temperature of the sample gas was increased; the signal was found to decrease. This was attributed to adiabatic heating of the gas in the PM cell.

At the peak of the compression cycle the temporal temperature of the gas was greater than ambient, possibly greater than that of the gas in the sample cell. At the peak of the rarefaction cycle the gas temperature was lower than ambient. Under these conditions the gas in the pressure modulator cell was behaving as a dominating temporal radiator instead of a passive temporal wavelength.filter. This characteristic of the pressure modulator cell was not investigated further in part 1 of the program.

1.4 SUMMARY OF TASK 3

A new optical system was built around the design of one section of the MAPS optical system. An InSb detector with a sensitive surface 2 mm x 2 mm square was purchased and a 20 cm sample cell and 4" x 4" square black body was provided by Langley. The system was assembled, aligned and tested.

1.5 SUMMARY OF TASK 4

The sample cell and its ante-chamber were used to simulate the upwelling radiance from all CO molecules in the atmosphere. The optical properties of gases in the atmosphere are characterized by several parameters. One of the more important is the 'optical depth' of the gas: this is defined (for a homogeneous path) as U where $U = Cp\ L$ [C is the gas concentration; p is the pressure (atm) and L is the path length]. It is possible to simulate the optical depth for a long path in the atmosphere for a gas at a very low concentration (e.g., parts per million) with a short optical path in the laboratory.

This was the objective of this task and the results obtained were used to derive an equivalent weighting function for CO in the atmosphere at concentrations of 80 ppb; 100 ppb and 120 ppb.

1.6 SUMMARY OF TASK 5

The modulation of the upwelling radiance from the earth and atmosphere at frequencies between 2 Hz and 50 Hz was simulated. The earth's surface radiance was simulated by using a 4 inch square aperture black body maintained at 72°C. The time varying radiance component was generated by a hot wire stretched across the black body aperture. The temperature of the wire was cycled between two temperature limits through the AC current that was passed through it. The results of this experiment indicate that the PMR output will be relatively insensitive to a scintillating earth background.

1.7 SUMMARY OF TASK 6

The interference between the CO and N_2O species was investigated by using N_2O in the modulator cell instead of CO. The magnitude of the interference is not large; it is dependent on such parameters as the relative strengths of overlapping lines and the number of molecules in the optical path in the atmosphere and the position and width of the passband of the narrow band filter. Further experiments should be performed and computer calculations made, to evaluate the magnitude of the interference.

2.0 OVERVIEW OF TASKS 1 AND 2

A detailed description of the work performed in Tasks 1 and 2 is given in an interim report; only the more important aspects will be discussed in the next two sections.

2.1 TEST SYSTEM HARDWARE

An earlier experimental apparatus is shown schematically in Figures 2-1, 2-2 and 2-3. In Figure 2-1 the black body is the radiation source; radiation from it passes through the sample cell, the PM cell, the narrow band filter, and the lens onto the Insb detector. In the earlier experiments all the windows were made of uncoated silicon. These were later replaced with Irtran 2 material overcoated for high transmission. The silicon lens was eliminated and the Irtran lens was adjusted so that the BB aperture plane was again imaged on the detector. The sample cell had an integral temperature controlled water jacket; with this it was possible to maintain the sample cell at any temperature between room temperature and 75^{o}C. A full description of the PM cell is given in Section 3.2; the wavelength response of the optical filter is shown in Figure 2-4.

The processing electronics used for the background modulation experiments and PM experiments are shown in Figure 2-2. When the silicon windows of the sample cell and PM cell were replaced with Irtran, the 500 kΩ load was reduced to 10,000 Ω and the PAR 113 preamp was used between the detector load and Ithaco lock-in amplifier.

The sample cell and PM cell had separate pumping systems as shown in Figure 2-3.

2.2 EXPERIMENTAL RESULTS

2.2.1 PM System Tests

Some performance tests were made with the system: the results of the more important ones are shown in Figures 2-5, 2-6 and 2-7.

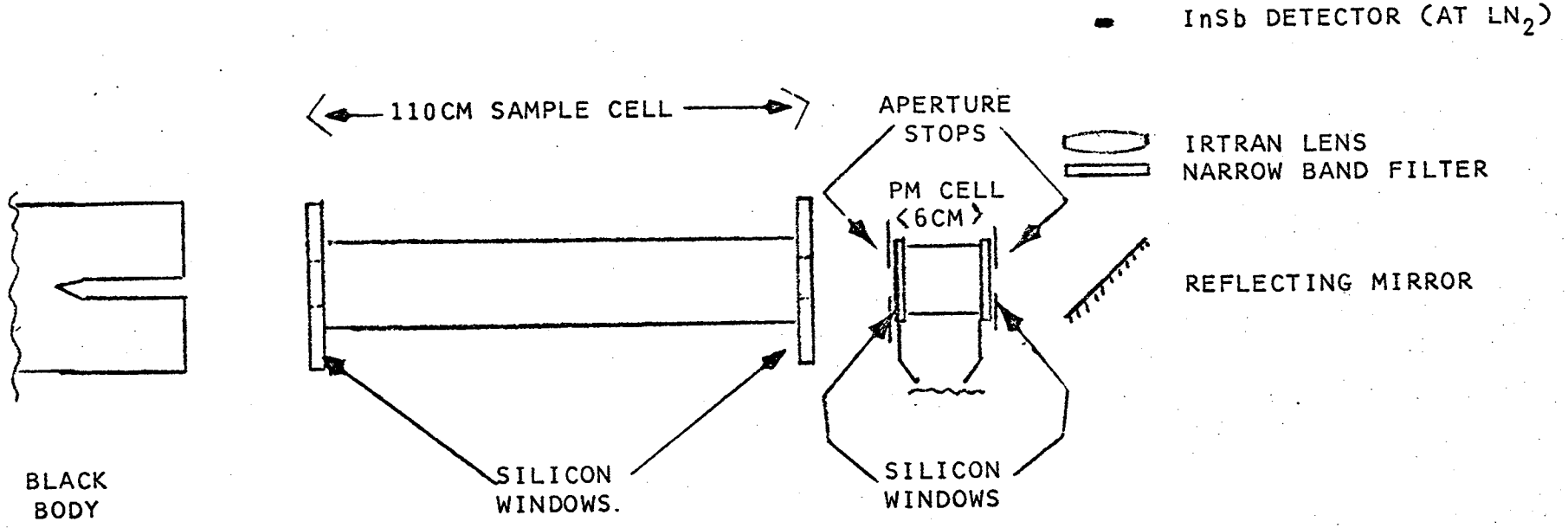

Figure 2-1. Schematic of the Original Optical System

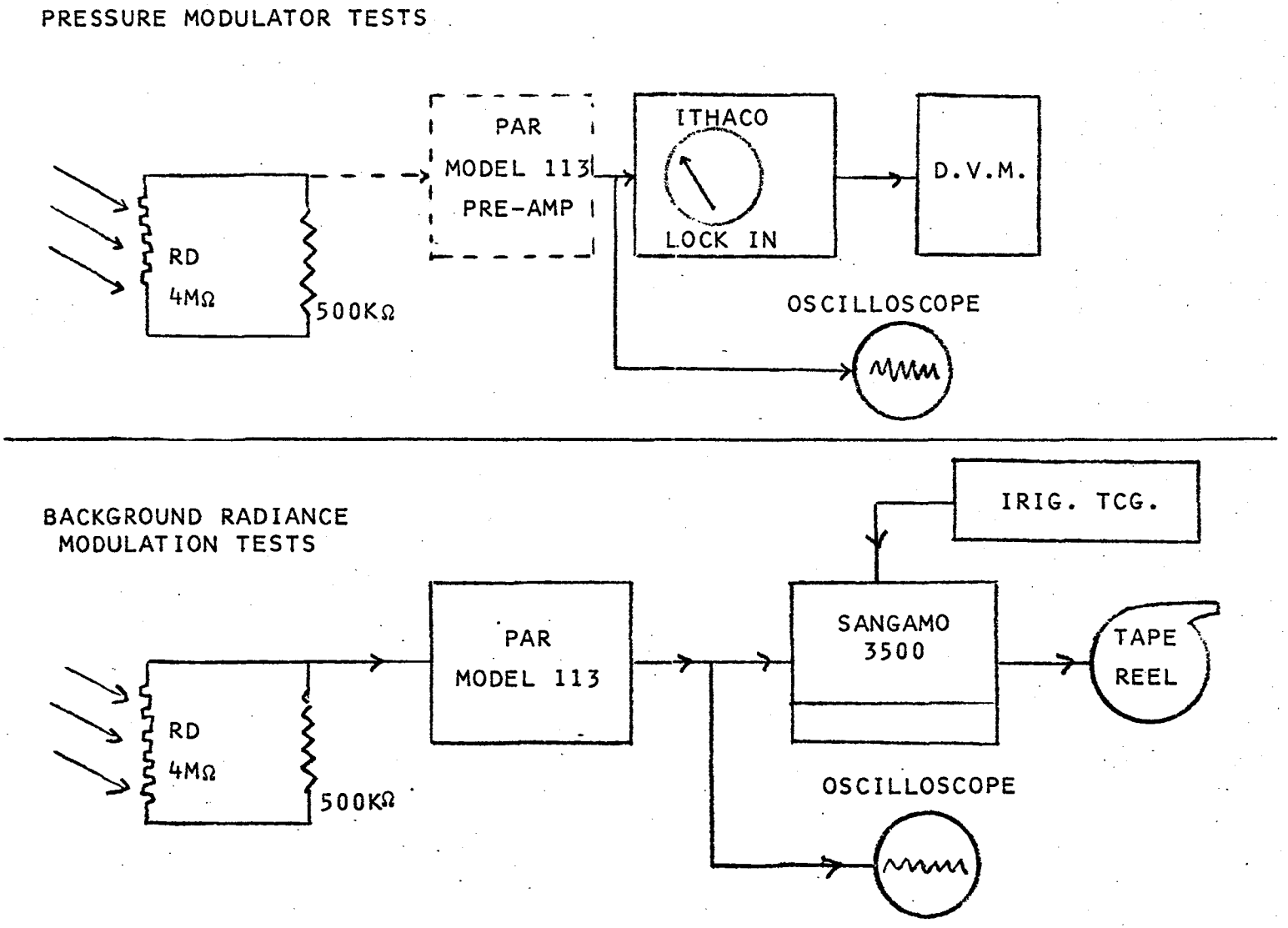

Figure 2-2. Signal Processing Schematic

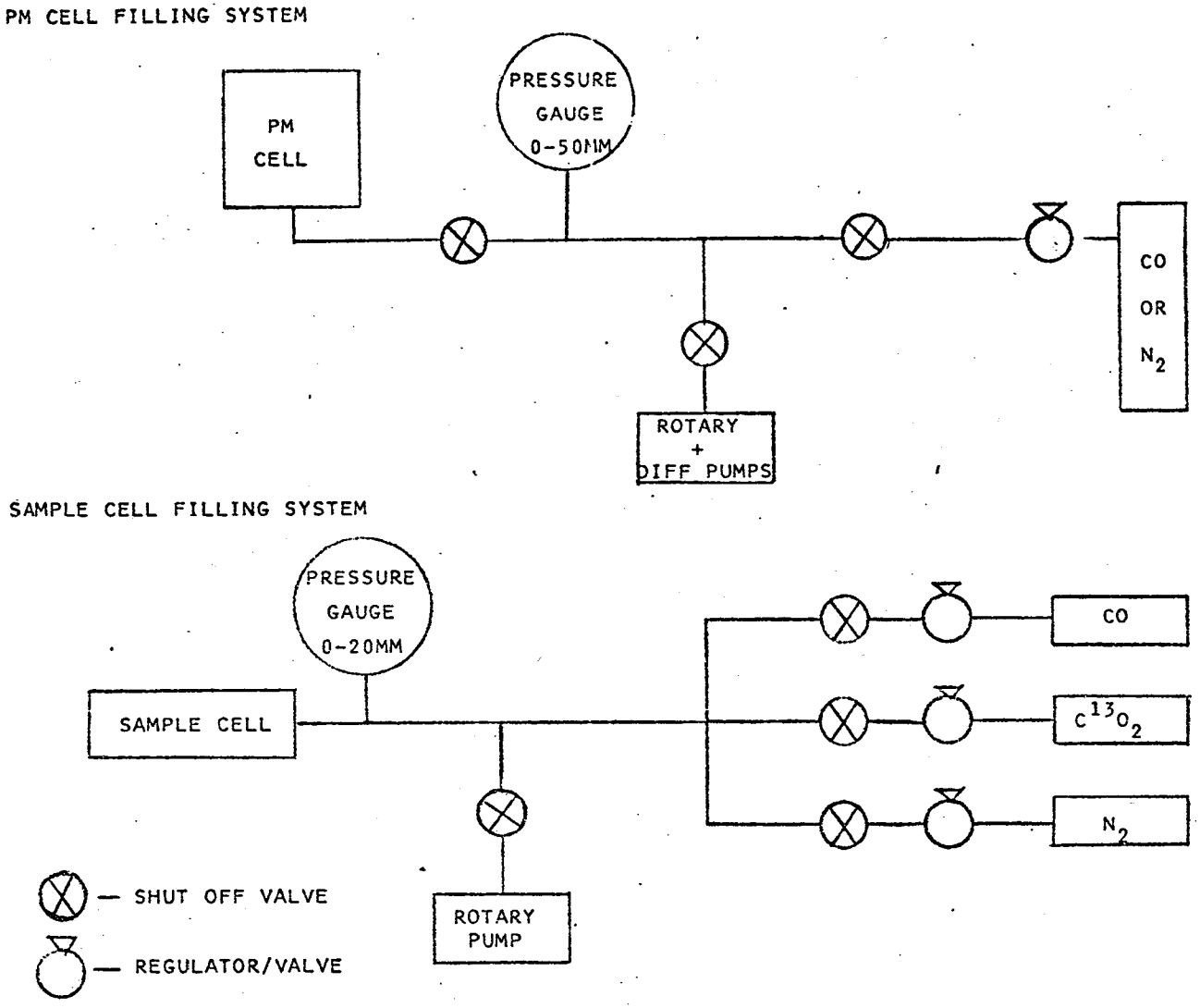

Figure 2-3. Pumping and Gas Filling Systems

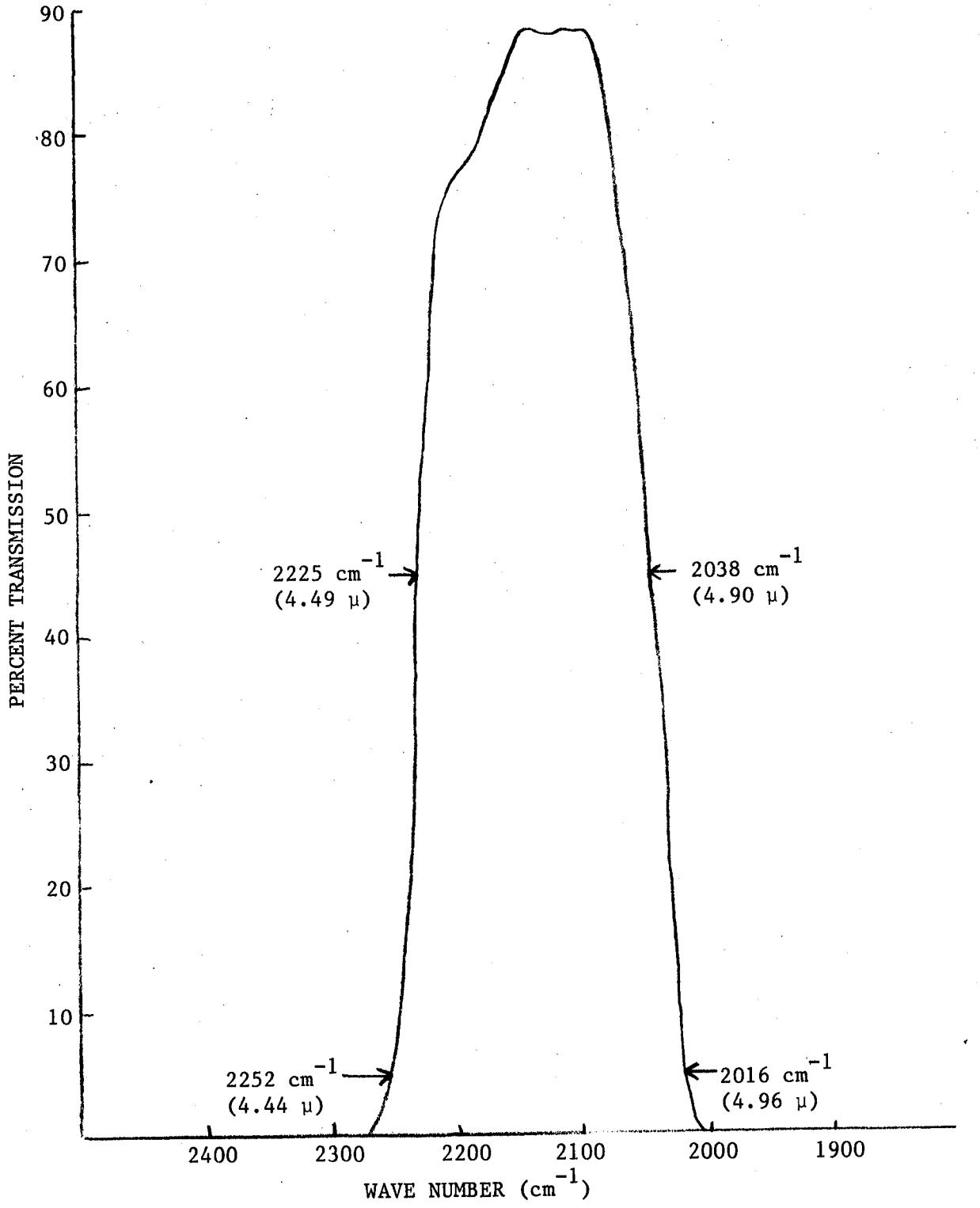

Figure 2-4. Passband Filter $\Delta\lambda$ = 0.41 μ

Figure 2-5 shows the frequency response of the PM cell as a function of the mean pressure in the cell; any gas can be used. The gradient of the curve shown is approximately 2 Hz per 2 mm pressure change. The resolution of the frequency counter used to monitor the frequency was 0.1 Hz; pressure changes of 0.1 mm could therefore be observed using this instrument when the PMC was shut off from the pumping system.

The drive circuit of the PM piston was power limited (1 watt max) and at a mean gas cell pressure of about 10 mm the amplitude decreased because of power limitation; this is shown in Figure 2-6. Carbon monoxide gas was used for these measurements and the background radiance was generated by the black body at about 200°C. Because the piston did not always start oscillating immediately at higher pressures, the cell mean pressure was maintained at a mean pressure of 8.8 mm Hg for future measurements.

The modulated signal decreases in amplitude as the background radiance decreases. At some background radiance the modulated output is zero. In Figure 2-7 this is shown to occur at a BB radiance of 100°C. The reason for such a high source temperature was not satisfactorily explained. Some adiabatic heating (and cooling) of the gas occurs but not of the magnitude indicated by Figure 2-7.

2.2.2 Measurements with a Modulated Background

The experimental system used for the background modulation experiment is shown in Figure 2-8. The sample cell was removed from the path between the PM cell and the black body. The PM signal at the detector load was amplified by the Ithaco Lock-In. The background modulated signals were amplified by the PAR 113 preamp and onto a fourteen track Sangamo 3500. The scope of the program did not permit the fabrication of a special chopper that gave the required low percentage (3-5%) modulation. The standard chopper supplied with the Brower Lock-In was used as an alternative.

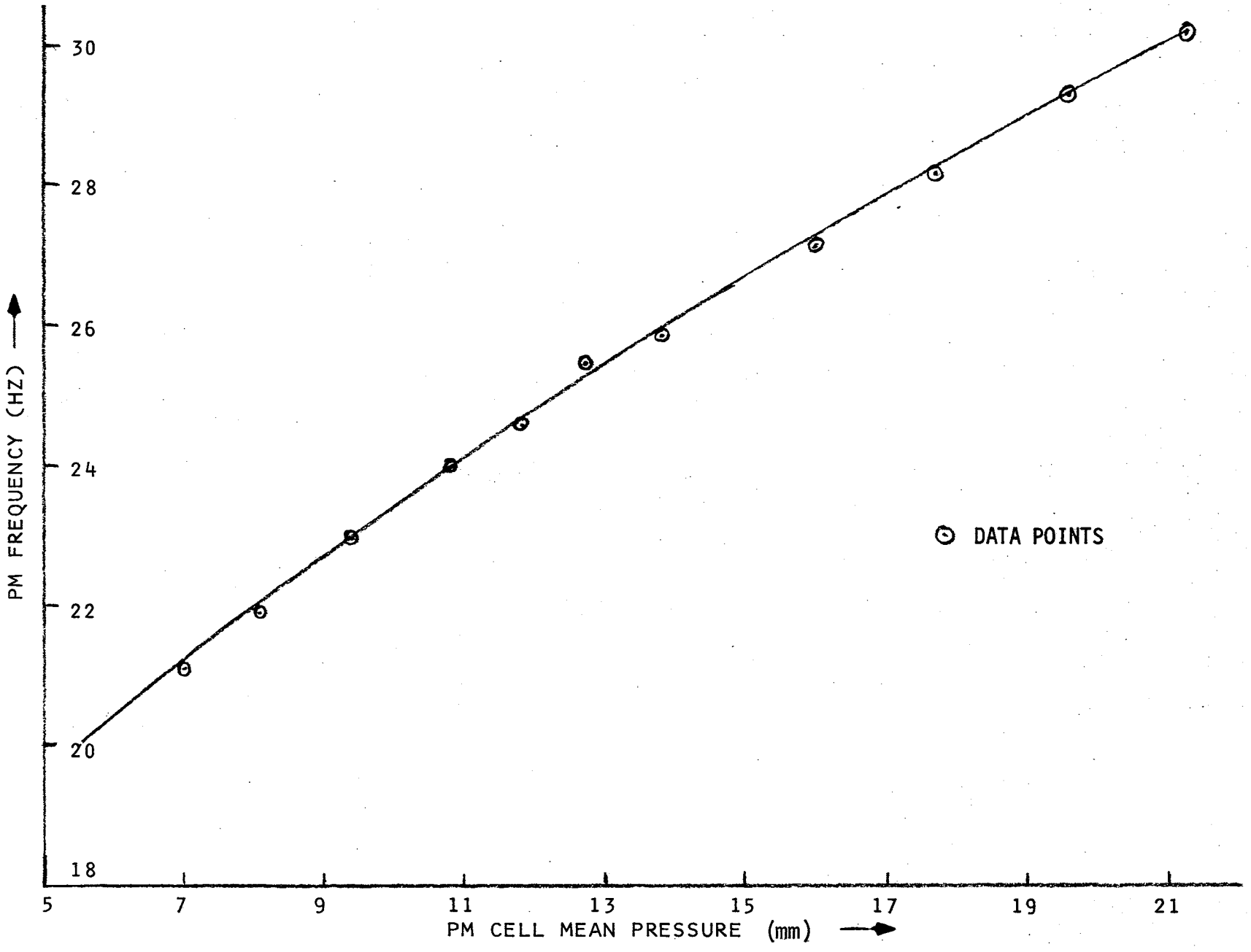

Figure 2-5. PM Frequency Vs PM Cell Mean Pressure

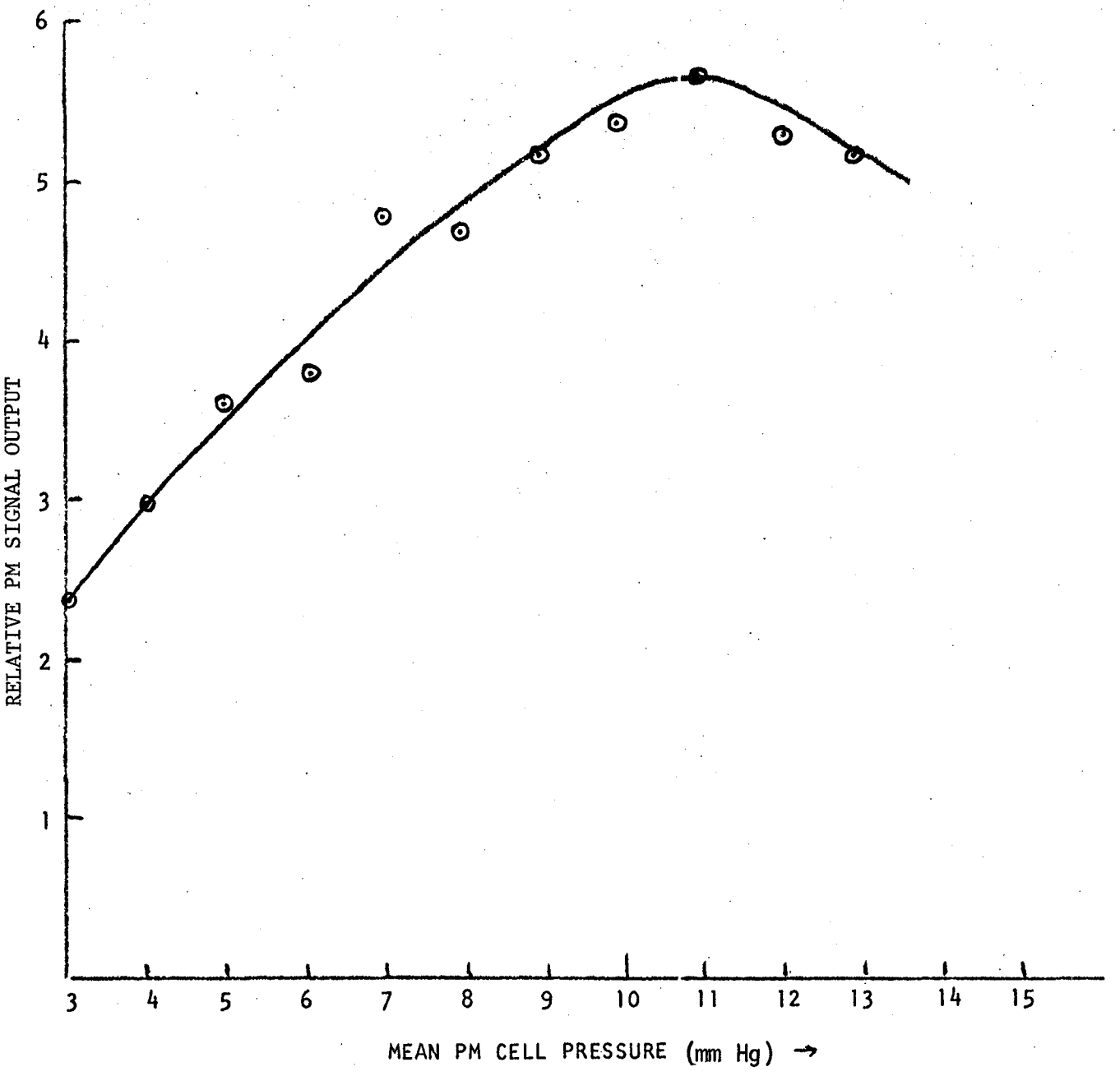

Figure 2-6. PM Signal Output Vs PM Cell Mean Pressure

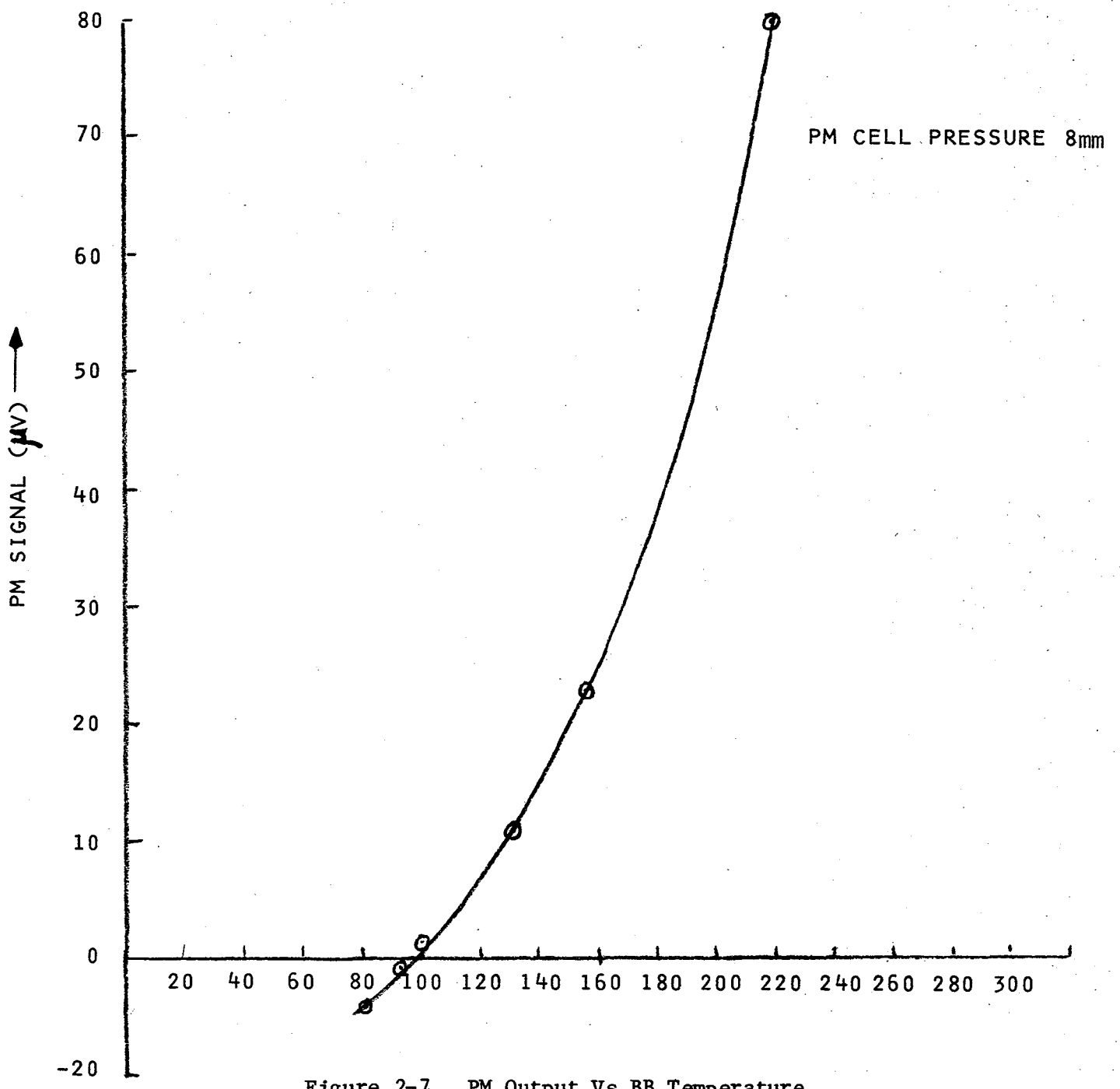

Figure 2-7. PM Output Vs BB Temperature

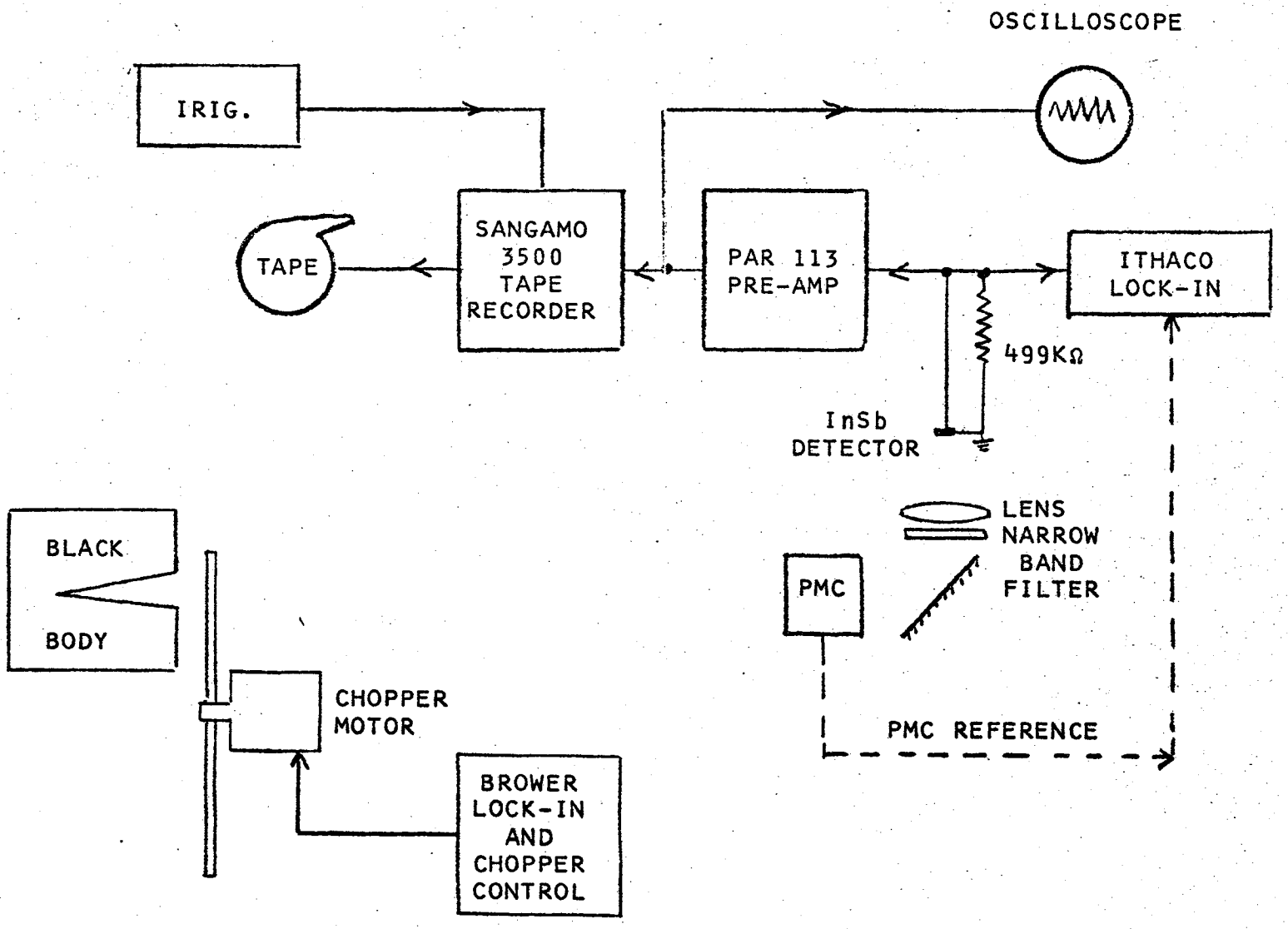

Figure 2-8. Experimental Setup for Background Modulation Measurements

The frequency of the chopper was varied from 1 Hz to 50 Hz. Several measurements were made near the frequency of the PMC and at fractions of a cycle from it. The randomicity of the phase between the chopped signal and the PMC had been confirmed by an independent experiment.

The magnetic tapes were sent to La.R.C. where they were reduced and analyzed. The results of the analysis confirmed that the percentage modulation was too high to provide meaningful results.

2.2.3 Measurements on Carbon Monoxide

No attempt was made to simulate the optical properties of the gases in the atmosphere with the available equipment in the laboratory. The sample cell was filled with 1 mm and 5 mm of CO and pure nitrogen gas was then added in 1 mm increments. The results obtained for the sample gas at room temperature are shown in Figure 2-9. These runs were repeated with the temperature of the gas cell raised in fixed increments to a maximum temperature of 75°C. The change in PM signal resulting from the increase in temperature is shown in Figure 2-10.

The interpretation of these results is as follows. The radiation from the black body is partially absorbed by the radiation in the sample cell over the (optically) chopped bandwidth range of the PMC. As the total pressure of CO in the sample cell increases, the absorption increases also, i.e., 5 mm of CO has a higher absorption than that for 1 mm. The greater the total pressure the larger the absorption of each individual line of the sample cell gas mixture.

When the temperature of the gas is increased the equivalent width of the individual lines remain the same for practical purposes but the self-radiance of the gas increases relatively rapidly with temperature. Therefore the total radiant power on the detector increases with gas cell temperature. Further results showing the signal dependence on temperature and gas concentration are shown in Figures 2-11 and 2-12.

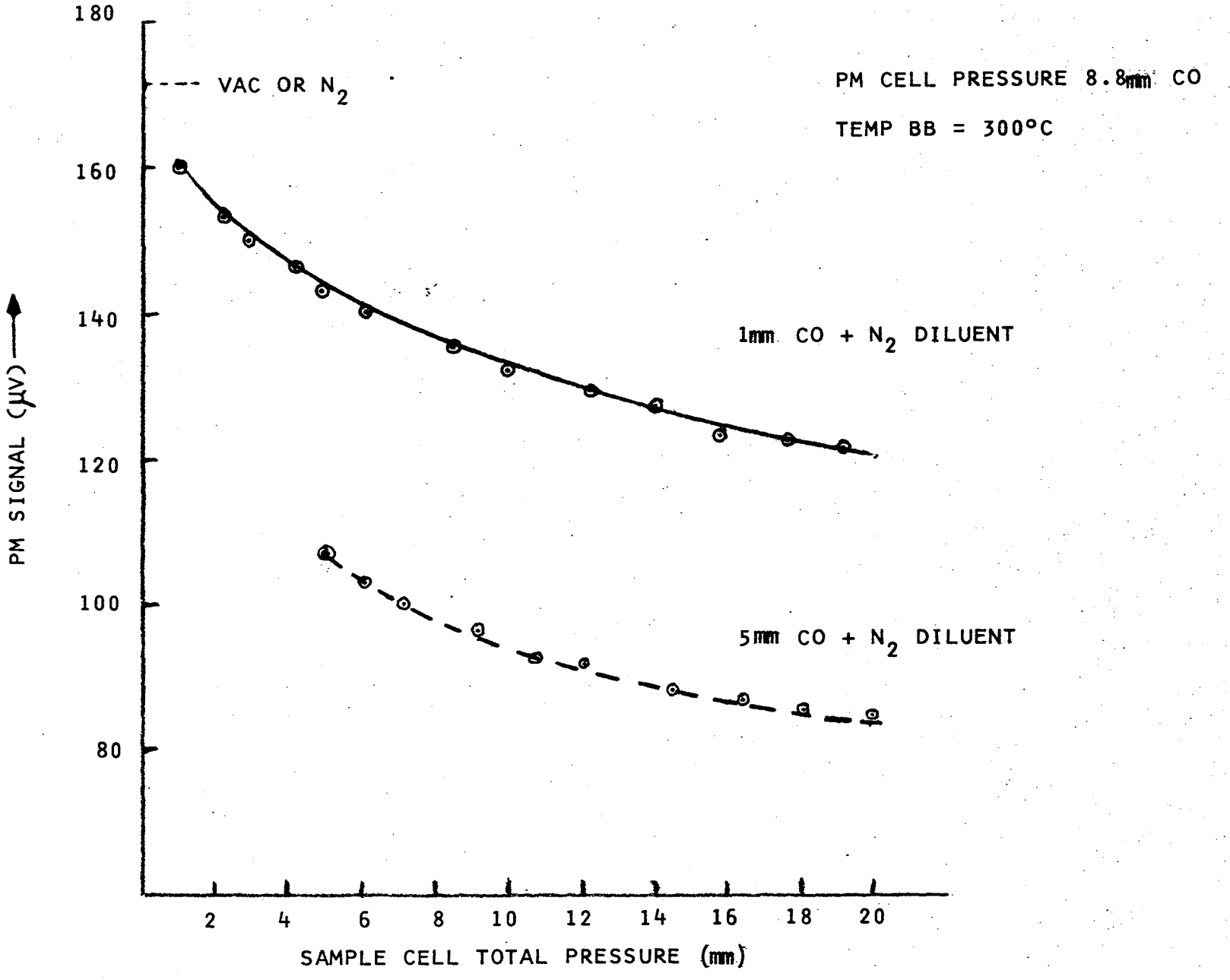

Figure 2-9. PM Signal Vs CO Concentration

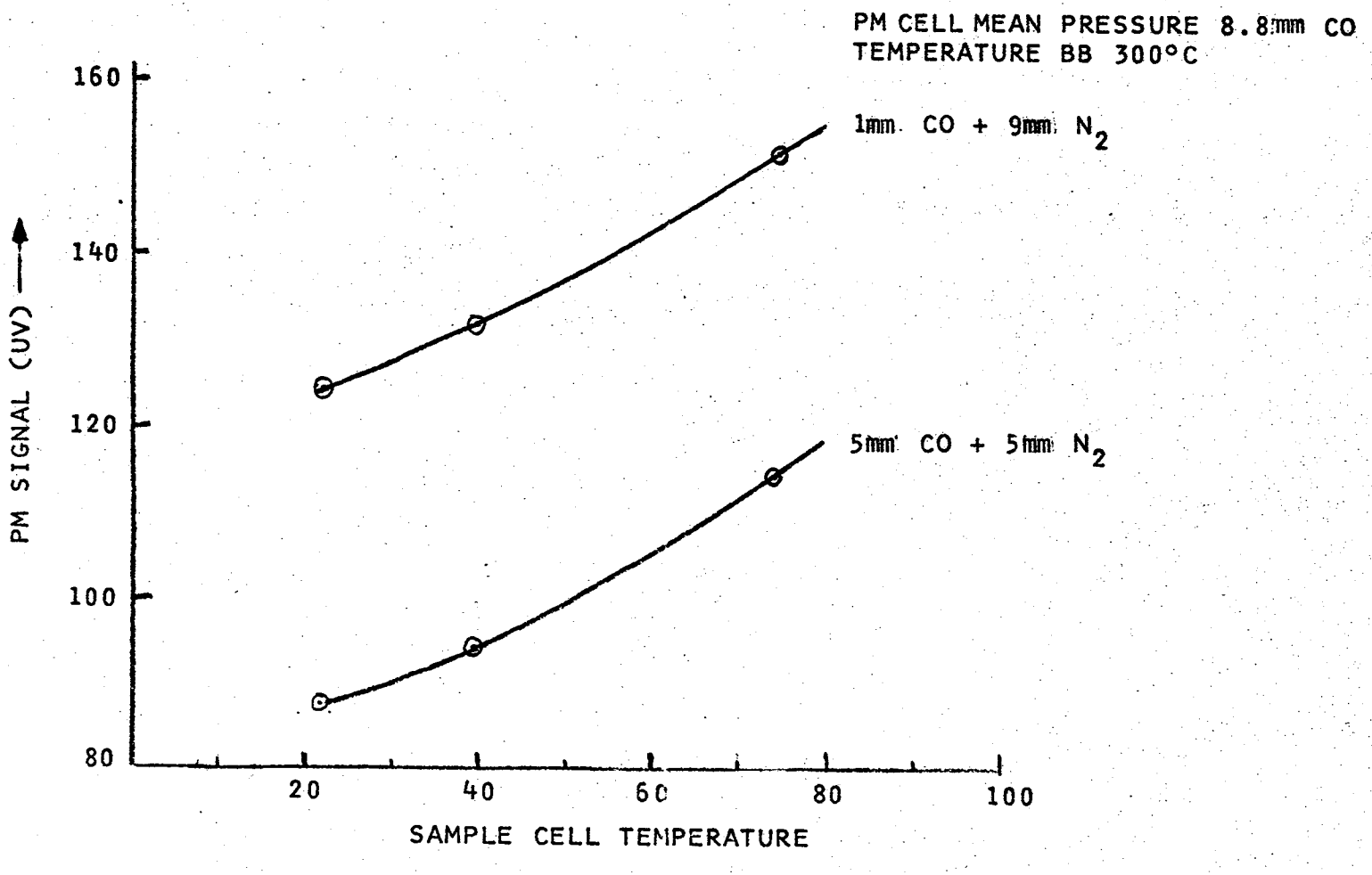

Figure 2-10. PM Signal for Constant Sample Cell Pressure as Function of CO Concentration & Temperature

2.2.4 Measurements on $C^{13}O_2$

The passband of the interference filter used in the experiments (2080-2240 cm^{-1} or 4.46μ to 4.8μ) is sufficiently broad to encompass some of the vibration rotation spectra of $C^{13}O_2$, which is one of the gases which can be used as a temperature monitor. The individual lines of this gas do not exactly coincide with CO but there may be some degree of overlapping in the wings of the lines. The possible effect this may have on the PM signal was briefly examined. Gas mixtures of $C_{13}O_2$ and N_2 and CO, $C^{13}O_2$ and N_2 were used in the sample cell; the PM cell contained 8.8 mm of CO as before. The upper two curves of Figure 2-13 indicate the degree to which the overlapping of the spectra causes an effect on the CO signal. The overlapping of the spectra can only be shown through very high resolution spectra in this spectral interval. Complete overlapping (or super positioning) of the lines is extremely rare, but the outermost edges or wings of the line do frequency overlap. The absorption in the wings is usually very low which is why the modulation is weak. However in this case the origin of the signal may also be due to a trace amount of CO in the $C^{13}O_2$ gas. For comparison the signal levels obtained with pure CO are also shown on the same curve.

The effect on the CO signal caused by $C^{13}O_2$ is more clearly shown by the third and fourth curves. The addition of 3.5 mm to the 1 mm of CO is quite marked and is of the order of 10-15%. Similar results are obtained at higher temperatures as shown on Figure 2-14.

2.2.5 Conclusions from the Results of Task 1 and 2

An improved experimental set-up is needed in order to evaluate the PM approach properly. The sample cell should be so arranged that weighting function for the atmosphere can be simulated. Improved optics and a combined detector pre-amplifier package are also necessary. In order to make meaningful background

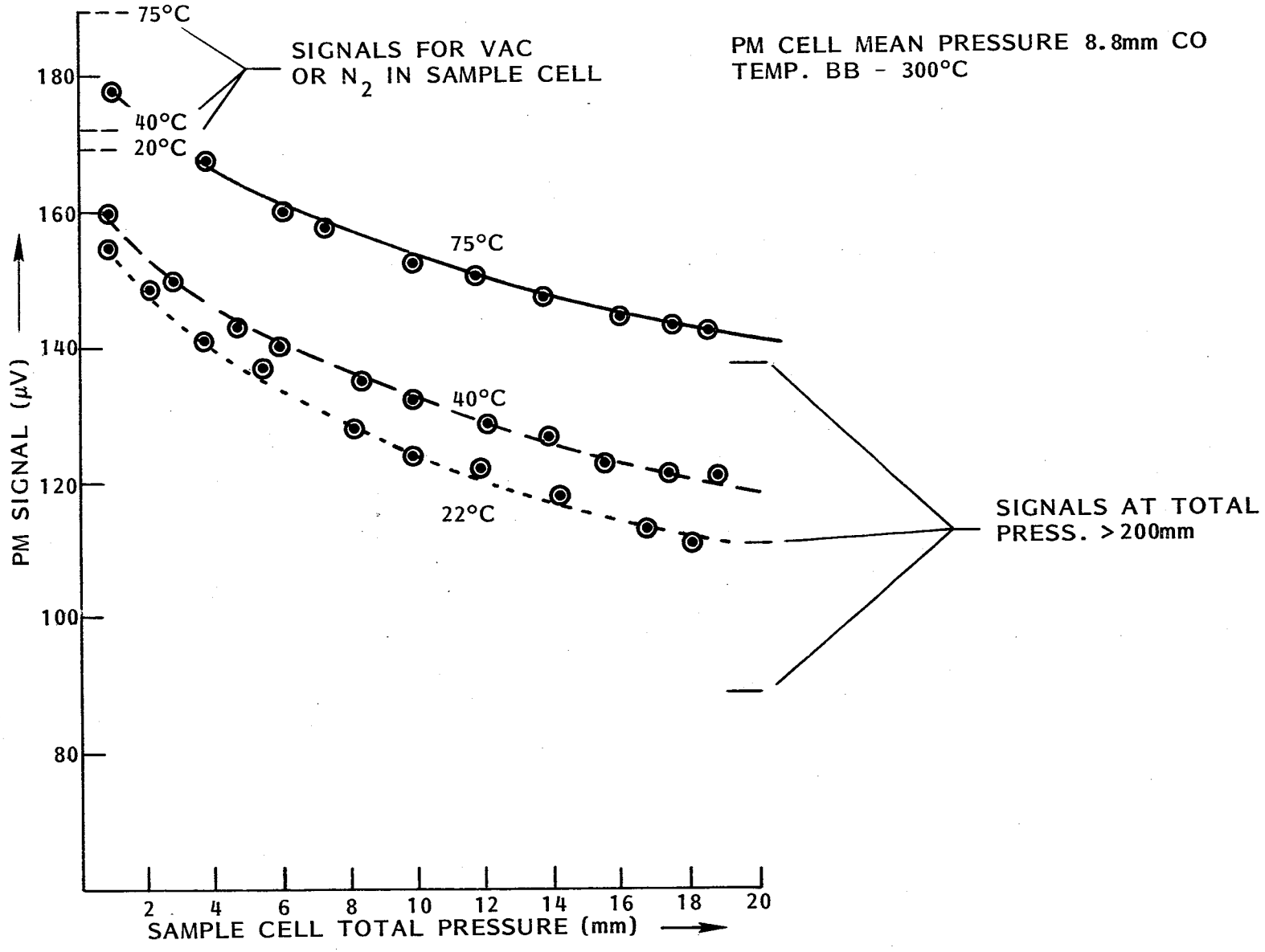

Figure 2-11. PM Signal for 1 mm CO + N_2 Diluent

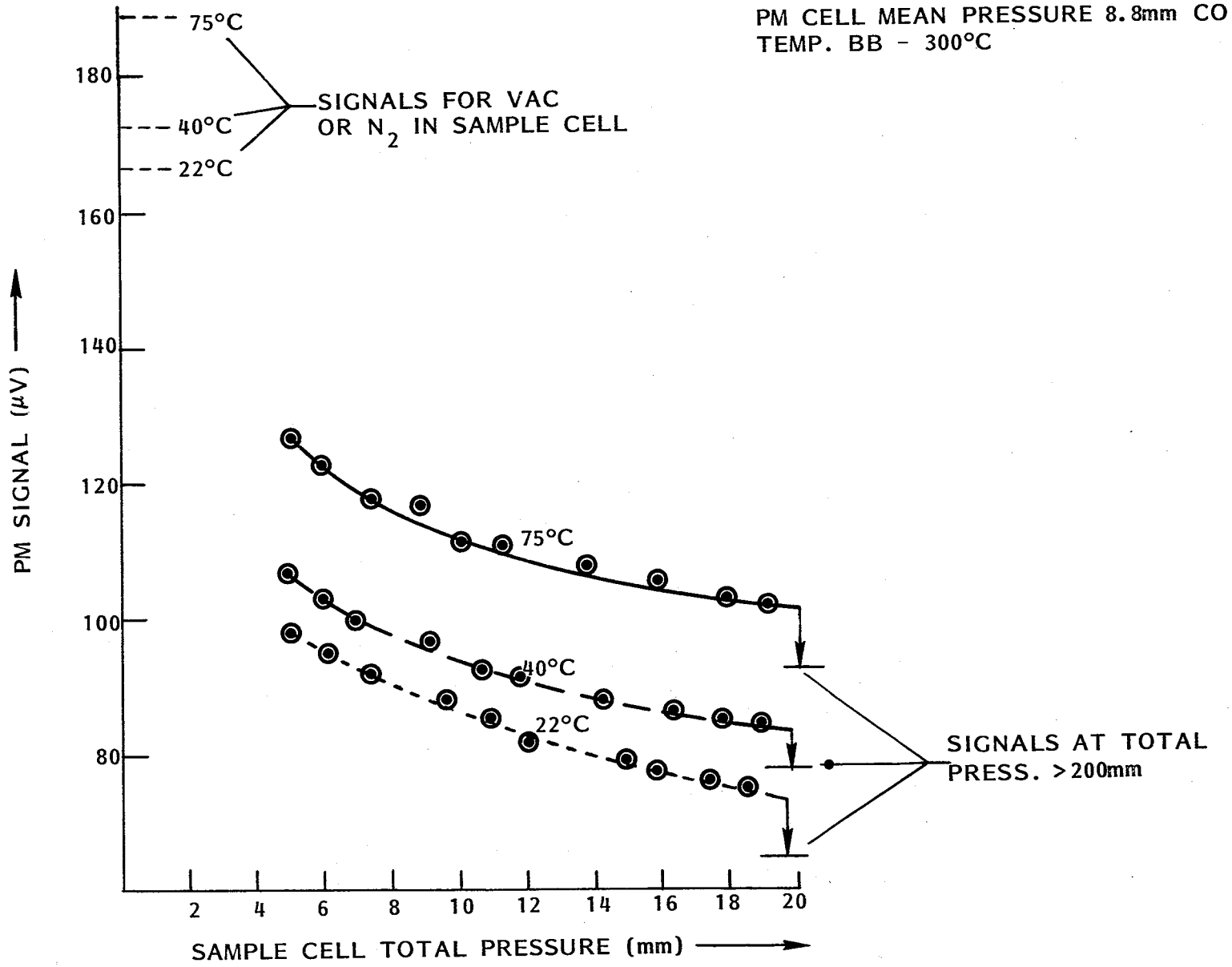

Figure 2-12. PM Signal for 5 mm CO + N_2 Diluent

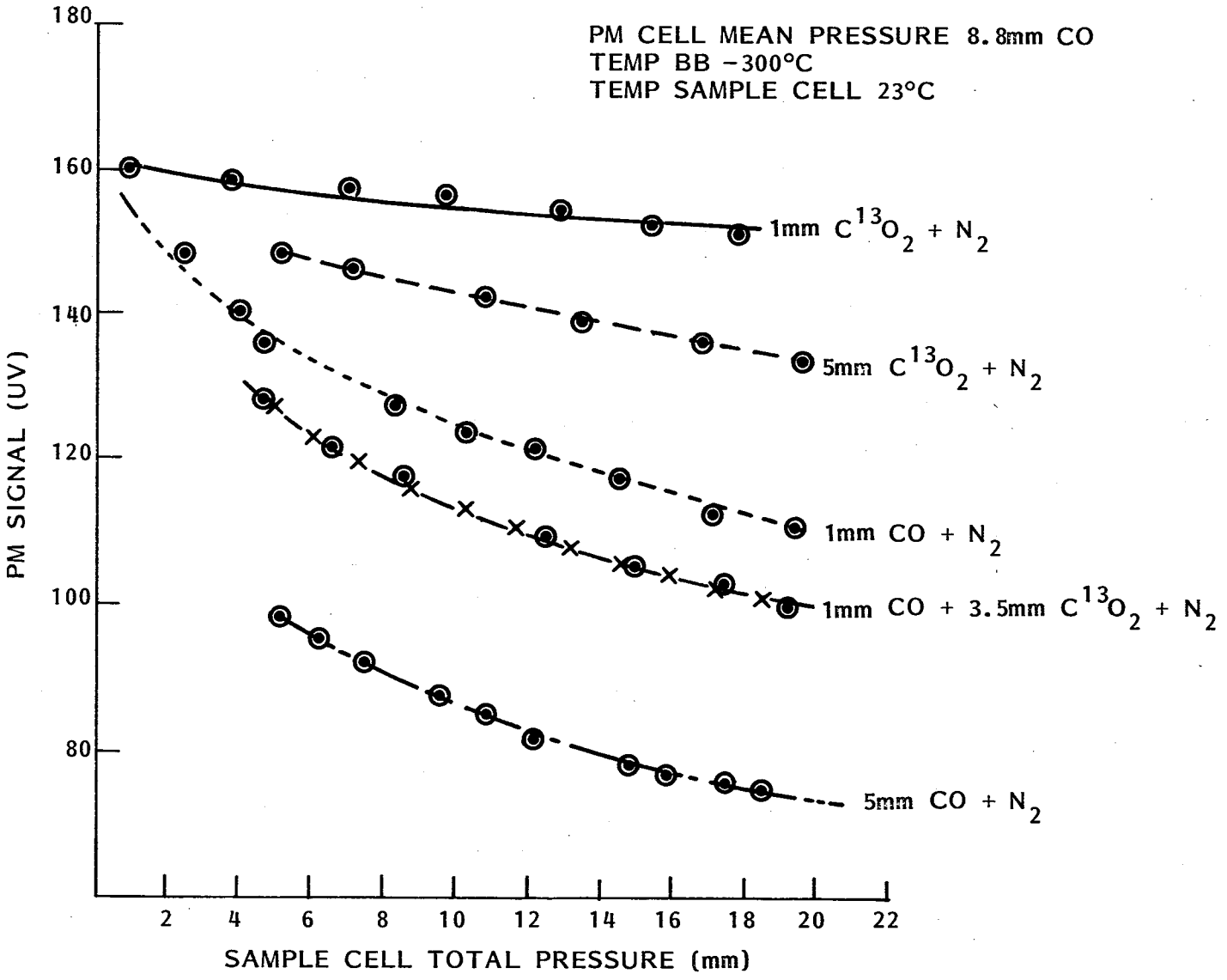

Figure 2-13. Comparison of PM Signals N_2 Diluted CO and $C^{13}O_2$

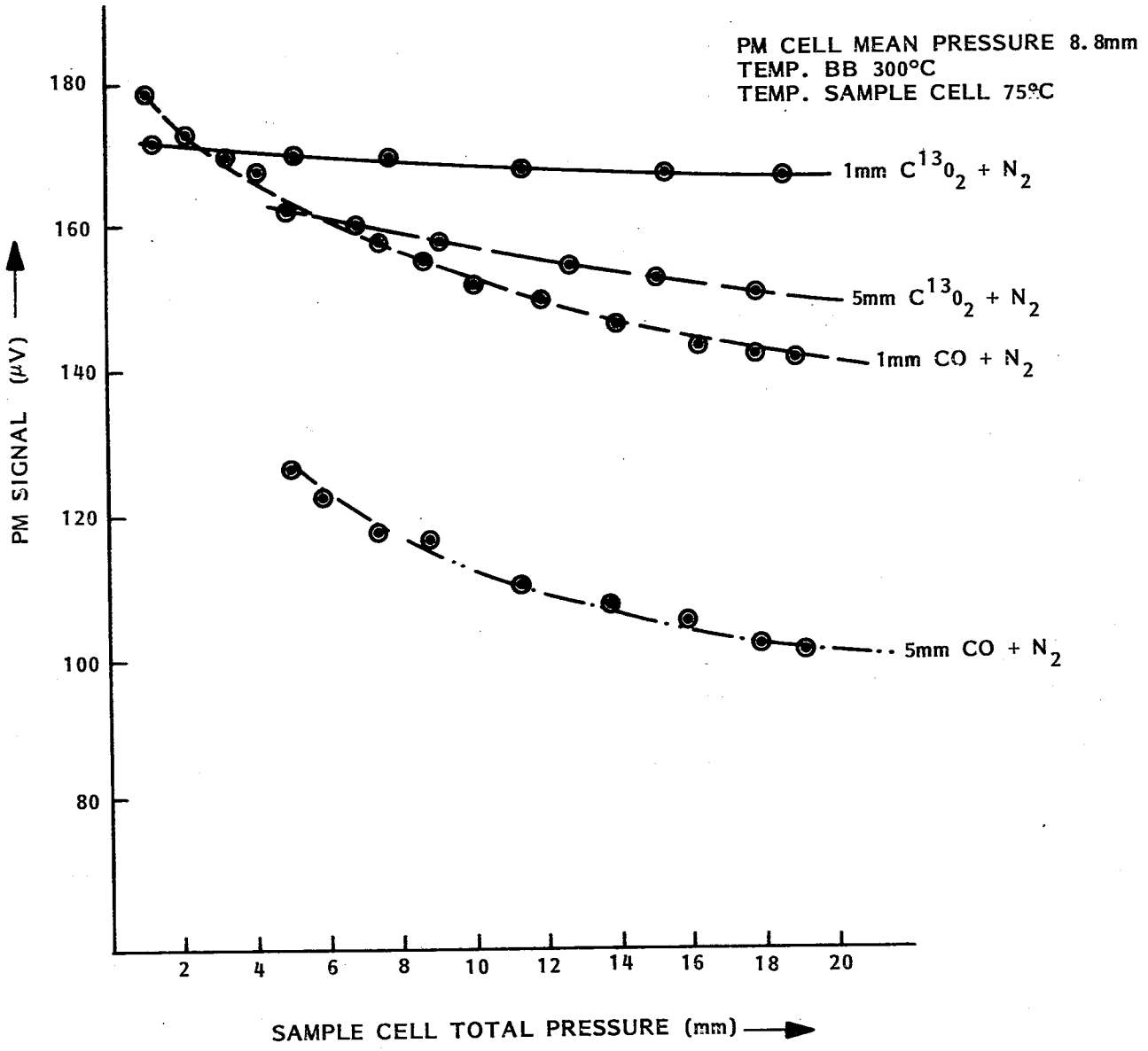

Figure 2-14. Comparison of PM Signals for N_2 Diluted CO and $C^{13}O_2$

modulation experiments a chopper having a beam occultation of only a few percent is required.

However, these tasks did demonstrate the dependence of the PM signal on gas concentration and temperature. The interaction of the CO and $C^{13}O_2$ spectra must be investigated more carefully and the effect of the apparent adiabatic heating and cooling cycle of the gas in the PMC on the system sensitivity must be examined.

3.0 TEST SYSTEM MODIFICATIONS

3.1 INTRODUCTION

In the original and amended form of the follow-up program, Task 3 remained unchanged. In this task, a new optical system, new sample cell, new black body and new detector were to be used. The objective of these changes was to have a more sensitive optical system with which it would be possible to measure the simulated radiative properties of specific gases in the atmosphere. In parallel with these new features, some measurements on the operating parameters of the PM were to be made. In addition, the performance of the PM drive circuit was to be evaluated with the objective of increasing power to the drive coil, so that higher mean pressures could be used in the PMC.

The results of these activities are described in the following sections.

3.2 PRESSURE MODULATOR MODIFICATIONS

The Nimbus "F" Pressure Modulator with a 6 cm long optical head is shown in Figure 3-1. A section through the lower part (modulator section) is shown in Figure 3-2. The assembled PMC is about 6" high and 3" in diameter; the lower section of the modulator has a volume of about 85 cc and the optical head 23 cc. The maximum throw of the piston is 1 cm which results in a swept volume of 28.3 cm^3. This swept volume can only be achieved at very low mean gas pressures owing to power limitation of the piston drive circuit.

In order to attain a good PM signal the max/min pressure of the gas in the optical cavity should be of the order of 2:1. Measurements were made on the piston travel as a function of mean gas pressure. The measurements were made with the optical head replaced by an aluminum ring of 8 mm height (6 cm diam.) and sealed with a flat glass plate. The volume between the glass plate and the ring of the PMC is the same as that of the optical head. The piston head was then illuminated with a small source of light and the piston movement measured with a

Figure 3-1. Nimbus "F" Pressure Modulator Cell and Optical Head

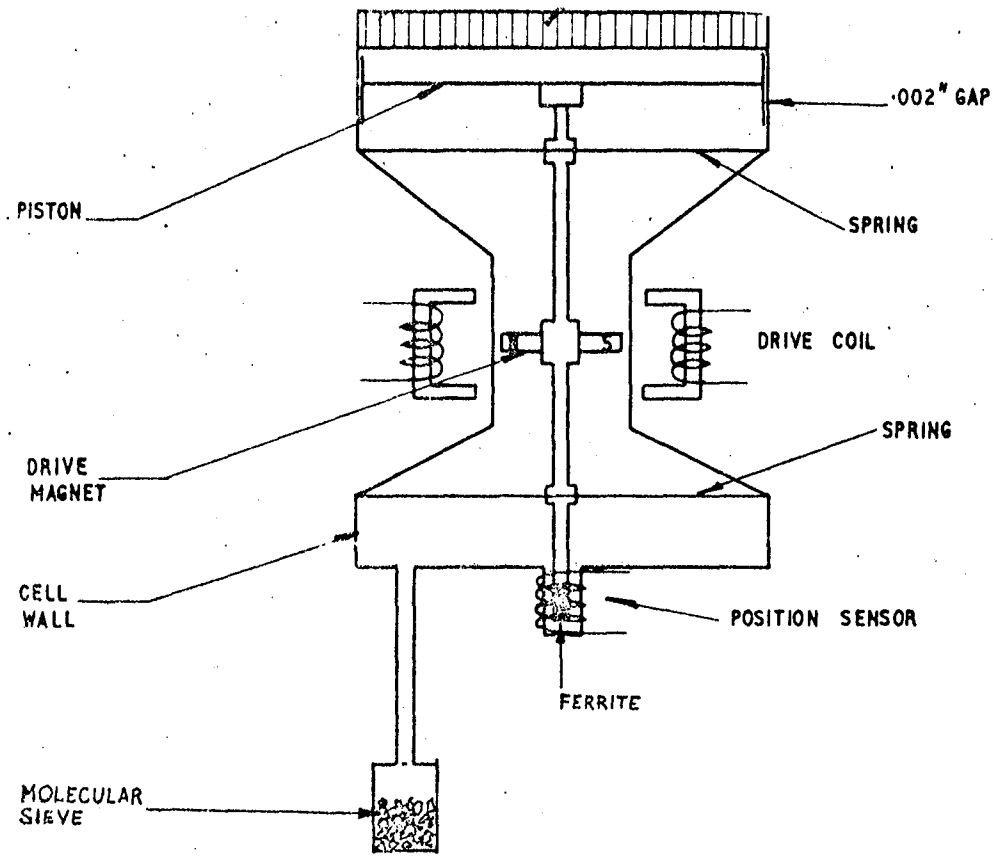

Figure 3-2. Section Through Pressure Modulator

traveling microscope; from these measurements the compression ratios were calculated.

There were two spacer rings; in addition to the one above, another with a height of 4 mm was used. This simulated the free volume of the optical head when some of the dead space above the piston was replaced by a solid disc of metal. The results of the series of measurements made are shown in Figure 3-3. These show that at the required mean pressure of 18 mm, the compression ratio would be about 1.1:1.

To increase the compression ratio, more electrical power was needed at the output driver to the PMC coils. This was accomplished by replacing the drive coils with a dummy load; the voltage across this load was then connected to the input of a stable power amplifier. The output of the power amplifier was connected across the PMC coils. In this configuration it was possible to apply up to nine times the output power of the original circuit in the coils. The circuit modifications are shown in Figure 3-4.

Test runs were made with the PM coils driven by the new power amplifier. An amplitude fall off at a pressure near 18 mm indicated that there was a power transfer limitation at the permanent magnet-PMC coil interface. In addition to this there was a measurable temperature rise in the outer parts of the PMC drive coils; the internal temperature could not however be measured. The external temperature recorded by an attached thermocouple is shown in Table 3-1. To avoid a possible breakdown of the coil and unnecessary heat transfer from the coil to the PMC chamber, the coil was driven at a lower power. The power selected was such that the external surfaces of the coil did not exceed 30^{o}C. The mean PMC pressure that can be used under these drive constraints is of the order of 7.5 mm to 10 mm.

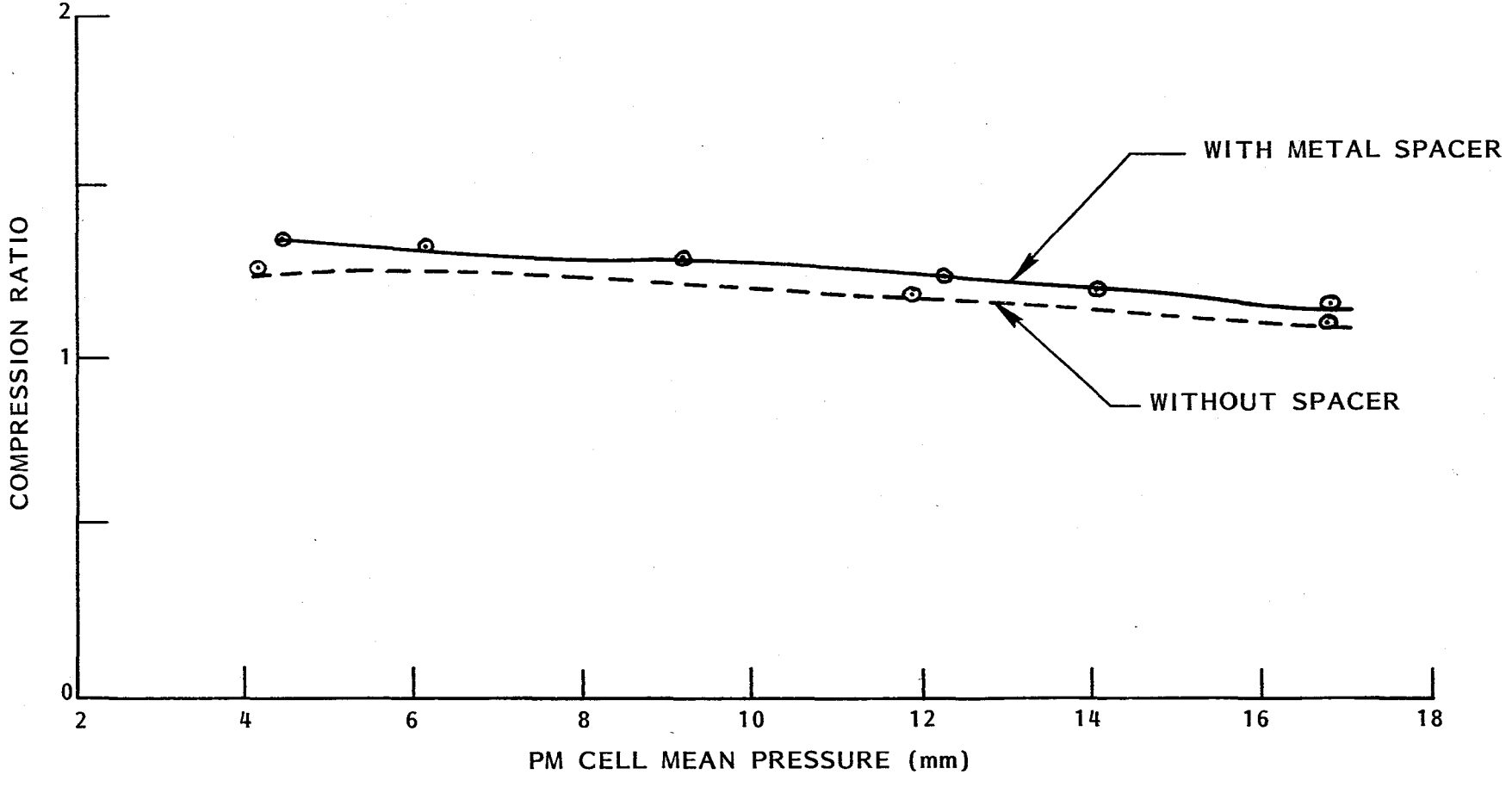

Figure 3-3. PM Cell Compression Ratio as a Function of Mean Pressure

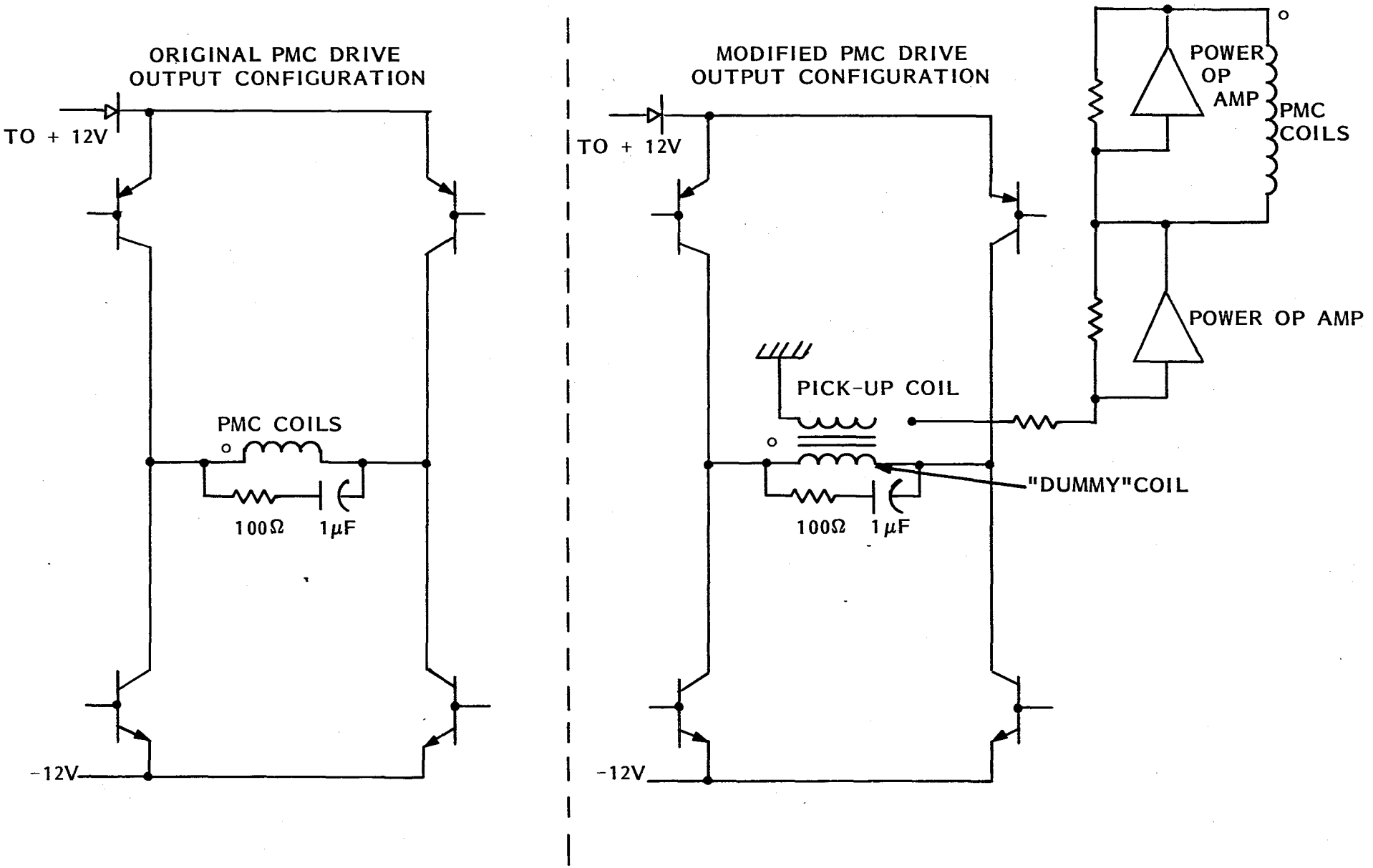

Figure 3-4. PMC Drive Modification

TABLE 3-1. PMC COIL TEMPERATURE VS TIME

Time (mins) After Start Up	Coil External Temperature °C
30	44
45	47.5
75	48
90	50

One final modification to the electronic drive circuits was made. An external voltage supply was connected to the circuit so that a fine adjustment to the amplitude of the piston could be made at a given power dissipation setting.

3.3 SAMPLE CELL AND EXPANSION CHAMBER

The sample cell is a straight cylinder 20.48 cm long between the inside faces of the windows; its internal diameter is 8.46 mm. Two 12 cm diameter windows are sealed onto each end by "O" ring seals. These windows are inclined at 3^{o} to the vertical to minimize the effects of internally reflected rays. Connected to the sample cell is an ante-chamber whose volume is about 15% of the latter. The sample cell volume is 1102 cm^3 and the internal volume of the ante-chamber can be varied between 132 and 220 cm^3 by inserting the appropriate metal plugs. The sample cell can be seen in Figure 3-8.

In use the sample cell is filled with a predetermined mixture of gases at a total pressure of 380 mm (Hg). The gases are allowed to mix for several hours. During the measurements the ante-chamber is pumped out between readings and the gas in the sample cell expands to fill the ante-chamber plus connecting piping and the volume of the pressure sensing device--a Baratron Type 77 pressure meter.

After the calibration run the Baratron is not used to measure the pressure at each pressure reduction; the average pressure reduction ratio is used instead. It was necessary to use it on the initial run because of the uncertainties in

the volume of the connecting tubing, valves, etc. The Baratron was selected primarily because the volume of its measurement chamber is only two or three cubic centimeters. The calibration curve obtained is shown in Figure 3-5; the mean pressure reduction ratio was found to be 0.854 and the maximum deviation from this figure was 0.002.

3.4 THE GAS FILLING AND PUMPING SYSTEM

The design of this system is a compromise between the requirements of good vacuum technique and those of the gas mixing system. It is shown in schematic form in Figure 3-6; a photograph of it can be seen in Figure 3-14. The meaning of the abbreviations used to describe the various values are as follows.

SCV - Sample Cell Valve
ECV - Expansion Chamber Valve
MRV - Main Roughing Valve
IV - Isolator Valve
PMV - Pressure Modulator Valve
PMHV - PM Hoke Valve
BIV - Baratron Interchamber Valve
BRV - Baratron Roughing Valve
MV - Micro-control Valve
G_1V - Gas 1 Valve
G_2V - Gas 2 Valve

The other abbreviations are:

PC - Pressure Chamber
RC - Reference Chamber
TCG - Thermocouple Gauge

The valve settings for the most frequently used functions are given in Table 3-2. The Baratron Pressure Meter measures the differential pressure between the reference chamber (which is continuously pumped) and the chamber open to the system. The pressure measured by this instrument is not therefore absolute

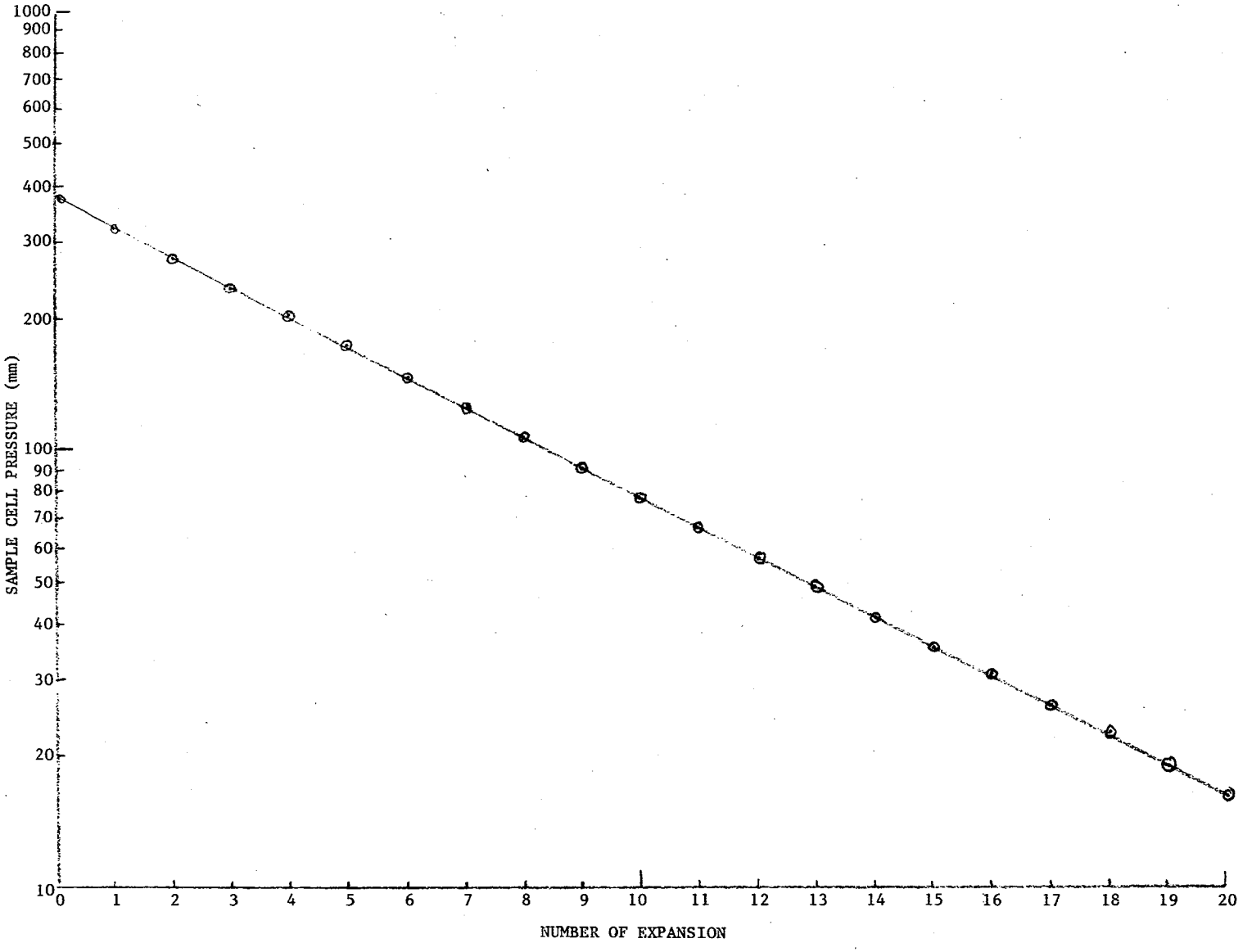

Figure 3-5. Sample Cell Pressure Vs Number of Expansions

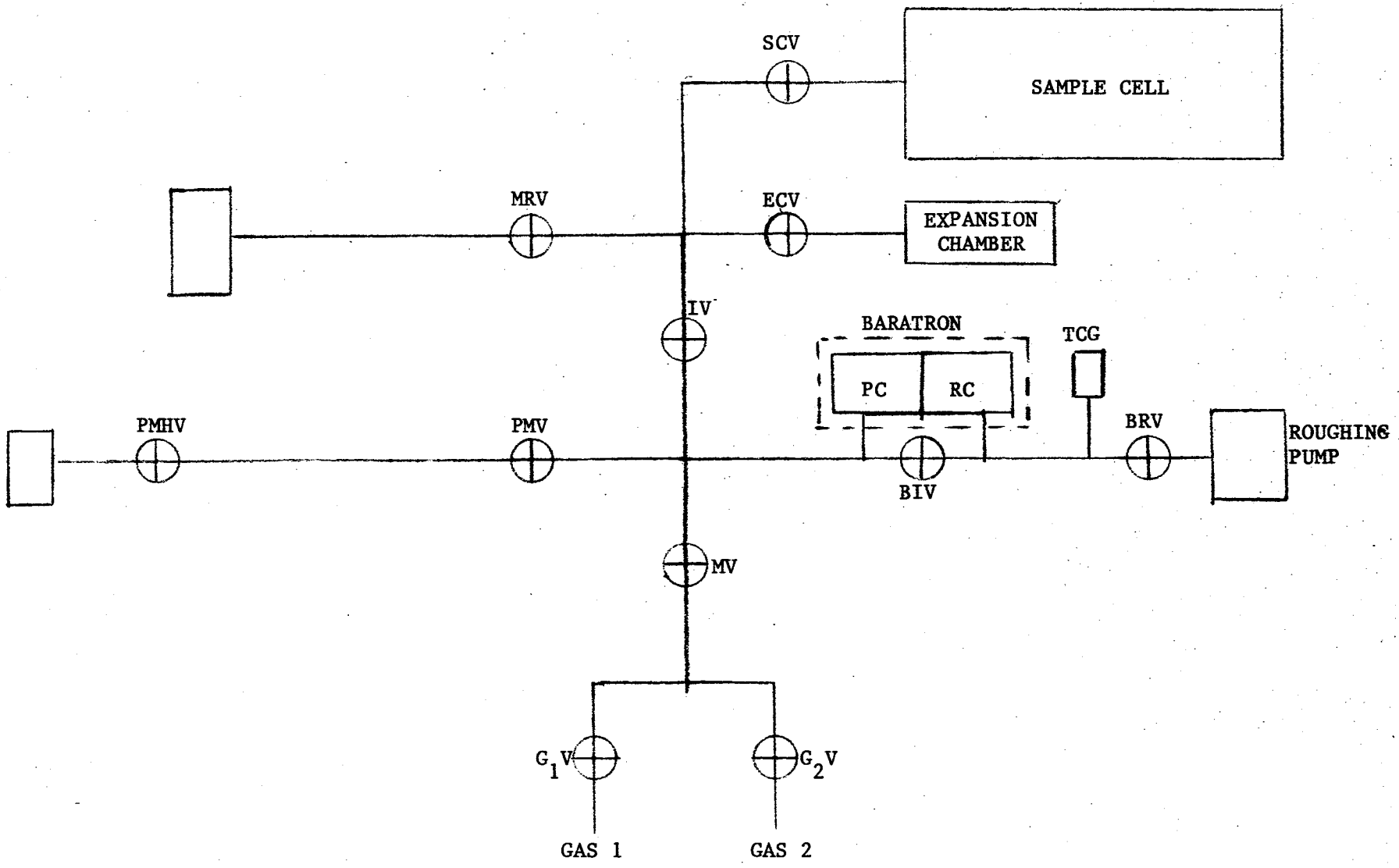

Figure 3-6. Gas Filling and Pumping System Schematic

pressure but because the vacuum reference is maintained at 10 microns (Hg) the error introduced is insignificant. In addition to the very small volume of the pressure chamber exposed to the system, the Baratron has the facility to measure pressures over the ranges from 0.1 mm to 1000 mm (Hg).

TABLE 3-2. VALVE SETTINGS FOR VARIOUS SYSTEM FUNCTIONS

Function	Valve Description										
	MRV	SCV	ECV	IV	PMHV	PMV	BIV	BEV	MB	G_1V	G_2V
System Pump Out	O	O	O	O	O	O	O	O	O	C	C
Sample Cell Pump Out	O	O	C	C	A	A	C	O	A	C	C
Expansion Chamber Pump Out	O	C	O	C	A	A	C	O	A	C	C
PM Pump Out*	O	C	C	O	O	O	C	O	A	C	C
Baratron Balance	A	A	A	C	C	C	O	O	C	C	C
Sample Cell Pressure Measurement	C	O	C	O	A	C	C	O	C	C	C
PM Cell Pressure Measurement**	O	O	O	C	O	O	C	O	C	C	C
System Gas Purge	C	O	O	O	O	O	C	O	O	O/C	O/C
Sample Cell Pressure Reduction	C	O	C	O	C	C	C	O	C	C	C
Expansion Chamber Pump Out	O	C	O	C	A	A	C	O	C	C	C

C = Closed; O = Open; A = Arbitrary (can be closed or open).

Notes: * For the initial pump out the PMC is disconnected from this system between PMHV and PMV and attached directly to a powerful pumping system.

** Normally PMHV is closed at all times after the PMC is filled and from this time on the PM Cell pressure is monitored by the PM frequency of oscillation.

3.5 THE SENSOR SYSTEM

The sensor system consists of the imaging system that collects and focuses the radiation from the source onto the detector. In order to minimize the cost of this item, the decision was made to use the design of one section of the Monitoring of Air Pollution System (MAPS). This system was originally designed for use at wavelengths from 4.6μ to about 9.5μ and for this reason all the components were made of germanium. In some respects it would have been more convenient to use Irtran 2, for example with this material alignment could have been done with an HeNe laser, but this would have required completely new specifications for the optical components. In the following sections the design, some analyses, details of the component fabrication and the assembly and alignment of the optical system are described.

3.5.1 The Optical Design and Specifications

These are shown for the imaging system in Figure 3-7. The objective lens focuses the scene (assumed to be at infinity) onto the plane of the field stop. This is a small circular aperture of 5 mm diameter; the image of the field stop is imaged by the relay lens onto a plane located about 1 cm in front of the field lens. The relay lens also images the objective lens onto the square-shaped aperture stop. The aperture stop is in turn imaged by the field lens onto the detector; in a perfect system the image of the aperture stop would be exactly superimposed on the detector element. The detector material is liquid nitrogen cooled Indium Antimonide and the size of the detector element is 2 mm square.

Between the aperture stop and the field lens, the ray bundle has the least convergence, and it is here that the PMC cells are situated. The 6 cm cell is shown in solid outline because this cell is the only one that was used. The planned position of the smaller cell (in phantom) that was to have been purchased

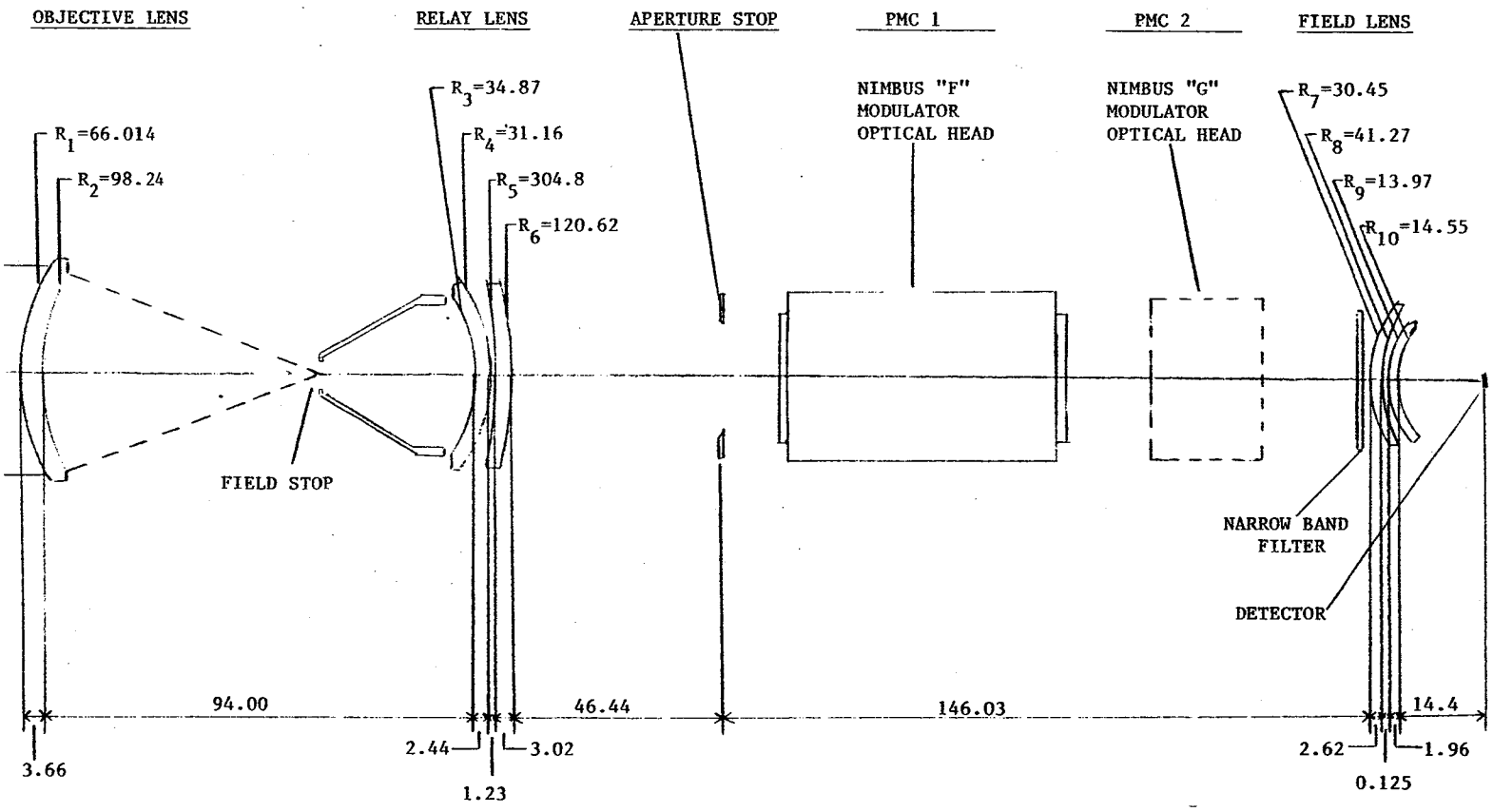

ALL DIMENSIONS IN MMS. REFRACTIVE INDEX OF ALL LENSES = 4.018.

Figure 3-7. Imaging System Design

and used in task 9 is also shown. The relative position of the imaging system, sample cell and black body are shown in Figure 3-8.

3.5.2 Fabrication

The lenses were manufactured by Exotic Materials Inc., California. All the optical surfaces were overcoated for a minimum transmittance of 97% at 4.6 microns. The appropriate MIL SPEC codes used were:

Surface Quality	MIL-C-48497
Humidity	MIL-C-675A, para. 4.6.9
Hardness	MIL-M-13508B, para. 4.4.5
Adherence	MIL-M-13508B, para. 4.4.6

Table 3-3 lists the specified dimensions of the components and the measurements that were made on their receipt. The tolerance was 0.1 mm for all dimensions except radii of curvature which were $\pm$0.1% for all components excluding the field lens for which the tolerance was $\pm$0.2%.

TABLE 3-3. GERMANIUM LENS PROPERTIES

Parameter	Lens #	Specified (mm)		Measured (mm)	
Diameter	1	50		50.09	
	2	35		35.05	
	3	35		35.05	
	4	28		28.02	
	5	23		23.03	
Radius of Curvature	1	R_1-66.091	R_2-98.298	R_1-66.014	R_2-98.24
	2	R_3-34.874	R_4-31.191	R_3-34.87	R_4-31.116
	3	R_5-304.8	R_6-120.498	R_5-304.8	R_6-120.624
	4	R_7-30.45	R_8-41.275	R_7-30.45	R_8-41.27
	5	R_9-13.97	R_{10}-14.549	R_9-13.97	R_{10}-14.55
Center Thickness	1	3.5		3.66	
	2	2.5		2.44	
	3	3.0		3.02	
	4	2.5		2.62	
	5	2.0		1.96	

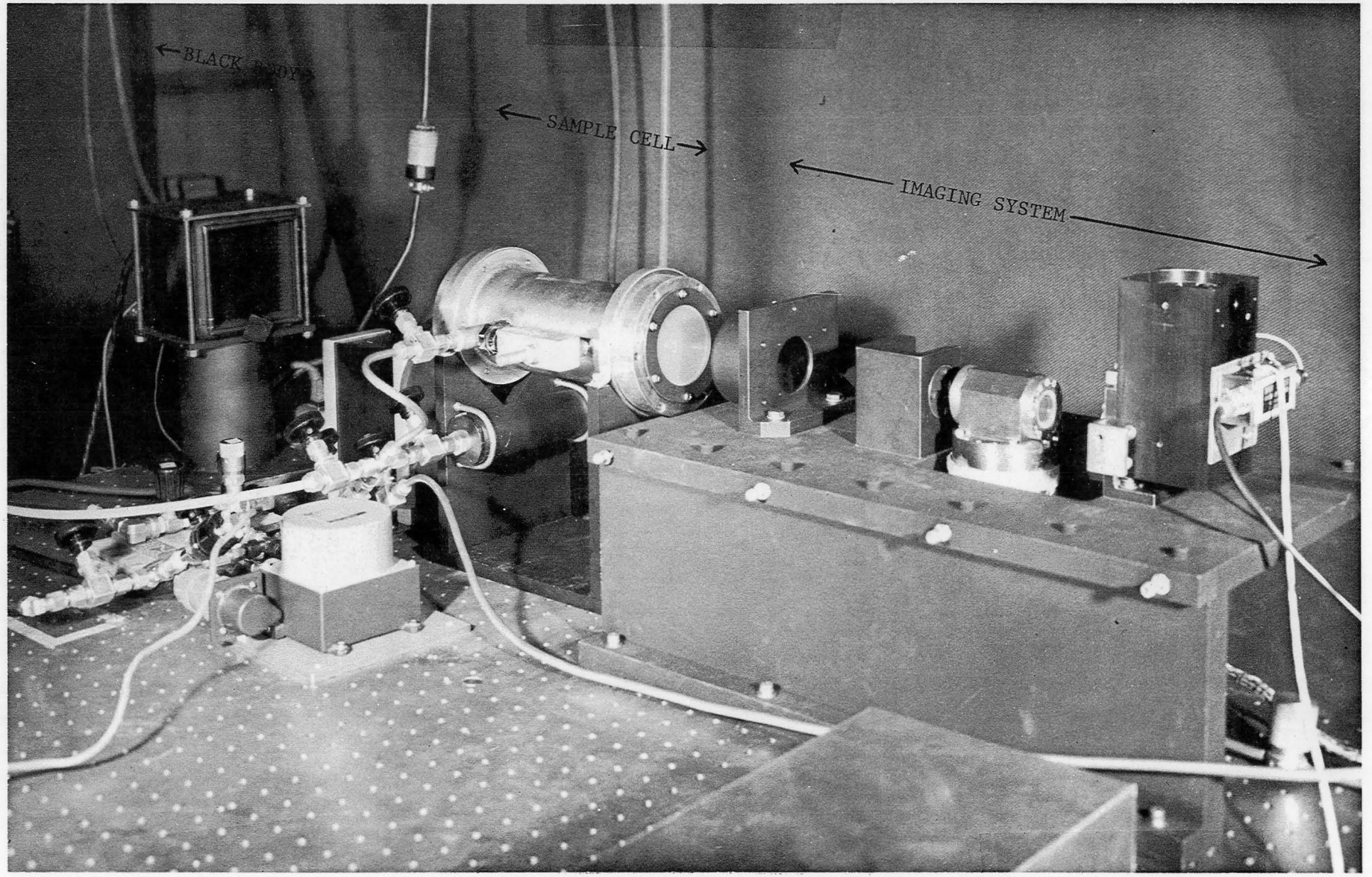

Figure 3-8. The Complete Optic System

The external transmittance of the lenses could not be measured in house, and the manufacturer's acceptance through their witness sample measurement was accepted.

The holders for the optical components were made to drawings supplied by La.R.C. These were mounted on a baseplate that raised the optical axis to 8½" above the base of the PM cell and coincident with the optic axis through the PMC optical head.

3.5.3 Alignment

There were three distinct stages of optical alignment; they were:

(1) The alignment of the imaging system components along a common axis.

(2) The axial positioning of the optical components.

(3) The alignment of the detector.

(1) For each of the optical components a blank metal disc with a 0.020" diameter hole at its center was made. The mounts for the individual components were positioned on scribe marks that had been made on the raised baseplate.

A mirror mounted to a 90^{o} angle plate was placed behind the baseplate as shown in Figure 3-9A. The alignment discs for the objective lens and field lens were placed in their holders and a laser was set up so that its beam passed through the two pinholes and were reflected back onto a pinhole aperture defining the laser beam. The discs for the other components were then placed in their respective holders and adjusted so that the beam passed axially through all of them.

The discs for the field lens and relay lens were removed and the lens, the element closest to the detector, was placed in its holder. It was adjusted to that the reflected beam formed a circle that was concentric with the pinhole in

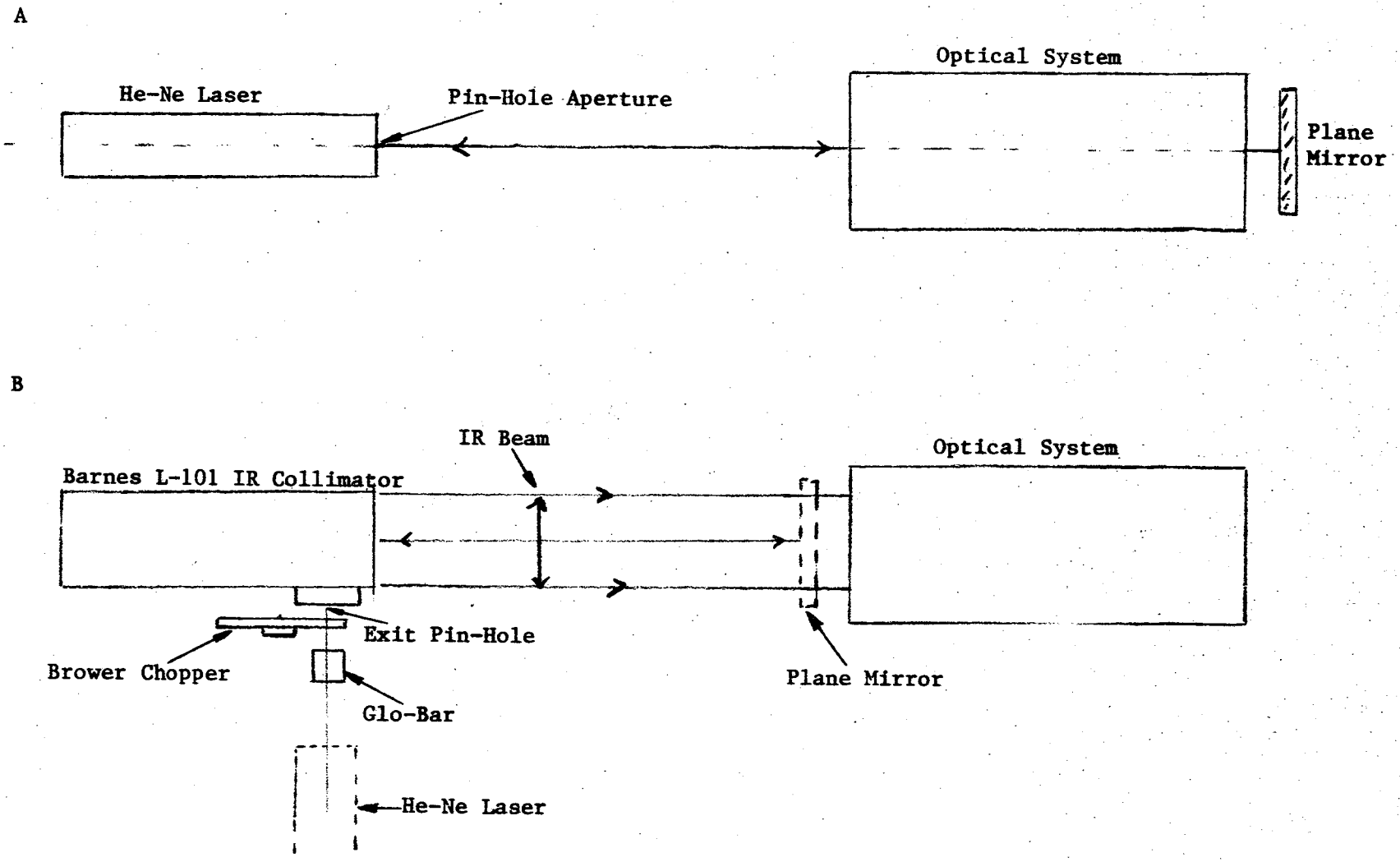

Figure 3-9. Optical Alignment Arrangements

the objective lens holder. This process was repeated for the second field lens component. The remaining optical components were aligned in exactly the same way with the exception that the objective pinhole was removed, and the circle of laser light was centered on the pinhole at the laser beam exit window.

With the imaging system components aligned the plane mirror was removed from behind the baseplate and moved to a position in front of it. Its face was adjusted so that the laser beam was returned along its own path.

(2) In order to place the optical components in their conjugate positions the arrangement shown in Figure 3-9B was used. A Barnes 6-107 (Reflecting) IR Collimator was mounted as shown. A small pinhole in a revolving aperture plate at the prime focus of the collimator was used to align the collimator axis parallel to that of the optical system. The laser was moved to the position shown and the collimator adjusted so that the beam was returned along its own path by the plane mirror (as before). The focus of the collimator was checked by illuminating a piece of diffusely transmitting paper with the laser beam to one side of the axial position. The returned image of the laser spot was found to be in sharp focus.

The laser was removed from behind the collimator aperture and replaced by a Globar/chopper combination as shown. The mirror was then removed from its position in front of the imaging system. An aperture of 0.008" diameter at the collimator focal plane was selected and illuminated from the nearby Globar. The angular subtense of the pinhole at the field stop of the optical system was calculated to be 0.3 milliradians in diameter. This is significantly smaller than the calculated blur circle diameter of 2.4 milliradians for the objective lens.

The final adjustments made were to set the Globar temperature so that a good signal (about 3 mV RMS) was developed at the detector preamp output, and to move the detector along the optical axis to find the position for a maximum signal.

The optical elements had been placed along the optic axis in positions calculated according to the specified properties of the optics. The final adjustments that had to be made were small because the manufactured components were very close to specification. The alignment measurements consisted of intercepting the bundle of rays within the imaging system with knife edges in the X-Y plane and noting the position of the knife edge that developed signals that were 90% and 10% of the maximum detector signal. The apparatus supporting the knife edges had to be able to transverse a linear distance of about 12" (Z direction), 3" in the horizontal (X axis) and about 2" in the vertical axis (Y axis). The measurement precision that had to be maintained in each axis was 0.001".

A jig was assembled from machine shop measuring instruments for this purpose; vernier gauges with a precision of 0.001" were used for the three axes. Using this jig the following measurements were made:

(1) Size of the blur circle formed by the objective lens.

(2) The position of the blur circle relative to the field stop.

(3) The position and size of the field stop.

(4) The axis of the optical beam relative to the geometric axis.

The shape of the convergent beam emerging from the objective lens near its focal plane is shown in Figure 3-10. Subsequent measurements showed that the image plane was 0.040" inside the field stop aperture plane; the objective lens was then moved forward by this amount. The center of the field stop was 0.006"

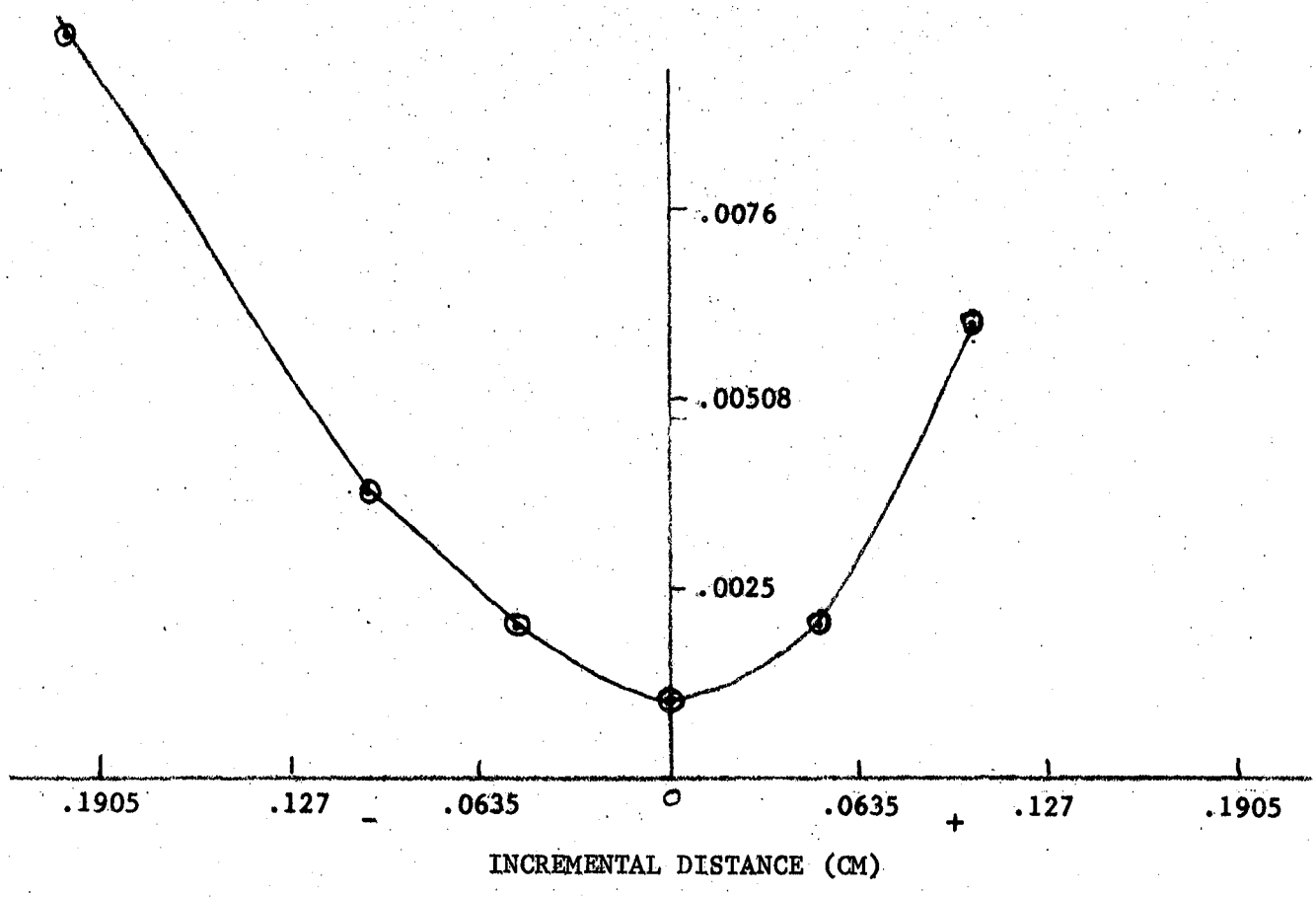

Figure 3-10. Image Diameter Vs. Position of Best Focus

above the center of the blur circle image. This was considered to be satisfactory because both measurements had errors of ±0.0025 cm. In order to define other properties of the optical system, the black body source was placed between the collimator aperture and the objective lens, this ensured that the optics was completely filled. The following results were obtained (all dimensions in centimeters).

Component	Horizontal Width	Horizontal Mid Point*	Vertical Width	Vertical Mid Point*
Front Face PMC	1.386	7.287	1.407	1.333
Back Face PMC	1.547	7.282	1.529	1.326
Image Plane of Field Stop	2.116	7.282	2.070	1.333
Field Stop	0.452	7.279	0.444	1.372

*Of the infrared beam relative to arbitrary positions of the measurement system.

These measurements span the entire length of the imaging system and show good symmetry of the ray bundle and position relative to the geometrical axis. The beam size external to the imaging system was also measured; of particular interest was the beam size in the planes of the front window and rear window of the sample cell. The measurements made in these two positions were more difficult to make and more inaccurate than the other measurements. They showed that near the front (closest to PMC) window the beam size is 3.175 cm x 4.445 cm and near the rear window 4.445 cm x 5.08 cm. The centers of the ray bundles through these image planes were 21.59 cm and 21.272 cm above the optical table. The height of the axis of the imaging system is 21.59 cm above the same plane.

(3) The final alignment was made to the detector; the image of the aperture stop is a 2 mm x 2 mm square that should overlay the detector element which was also 2 mm x 2 mm square. The detector mount had previously been set up for a maximum signal with an image size smaller than the detector. In this final adjustment the system was illuminated by the black body and with the optics filled, the image of the aperture stop and detector were of the same size. The detector was moved forward and aft of its position to obtain a maximum signal for the Z axis. The detector mount was then rotated about the optical axis to determine the maximum signal again. When this had been achieved, a final small adjustment was made along the Z axis.

3.6 SYSTEM INTEGRATION

As a part of the system integration subtask, a series of measurements were made on individual elements. Some of these had been done prior to the optical alignment, e.g., the detector sensitivity and noise measurements. The more important of these will be briefly described.

3.6.1 Detector Tests

The detector material is Indium Antimonide and the size of the detector element is 2 mm x 2 mm square. The detector is mounted in a glass dewar which is itself potted in an aluminum housing to which a Model 700 preamplifier is permanently attached. This unit can be seen in Figure 3-13.

Noise Equivalent Power (NEP) and D*

This measurement was to be used as a reference parameter; if any degradation of the detector or the preamplifier occurred it would be detected by repeating this experiment. The apparatus was set up as shown in Figure 3-11.

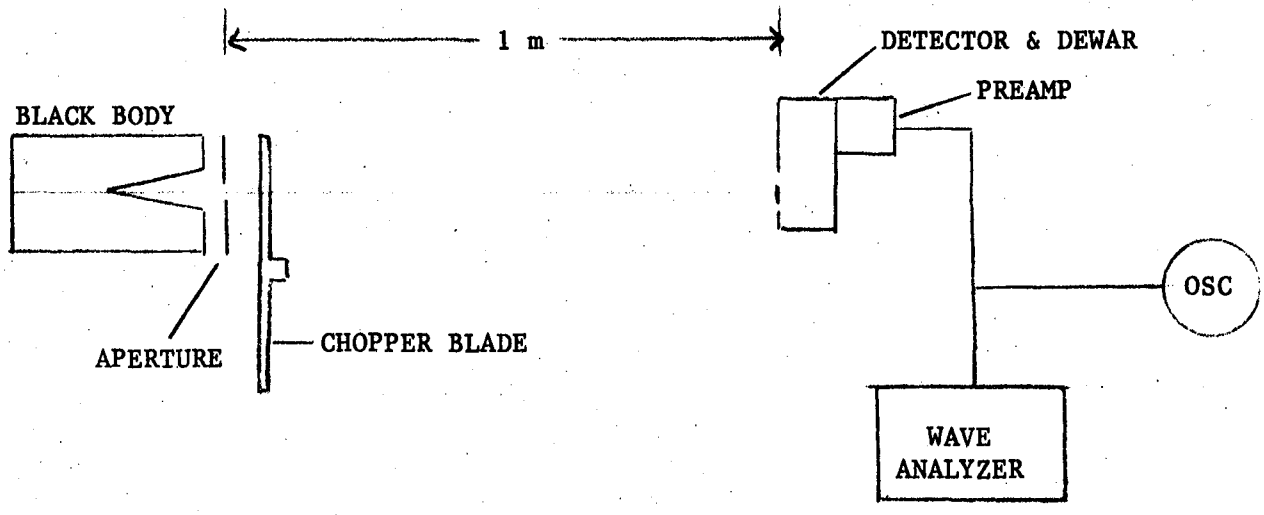

Figure 3-11. Detector D* Measurement

The black body was set to 500°K*; the apertures used were 0.05" and 0.1". The chopping efficiency of the aperture by the rotating blades was 0.44. The results were obtained by calculating the D* from the expression

$$D^* = \left[\frac{\Delta F}{Ad}\right]^{\frac{1}{2}} \times \frac{(S/N)}{Hd}$$

where ΔF is the bandwidth of the noise measurement (Hz); Ad the area of the detector (cm); and Hd is the detector irradiance (RMS watts/cm^2). The D*

*The black body used had been calibrated by the manufacturer only.

detector (cm); and Hd is the detector irradiance (RMS watts/cm^2). The D* obtained was 4×10^{10} cm $Hz^{1/2}$ $watts^{-1}$

This value of D* is typical for this type of InSb detector. The photon background (300°K) limited D* over the same spectral region is 1×10^{11} cm $Hz^{1/2}$ $watt^{-1}$.

The NEP is obtained from the detector D* by the expression:

$$NEP = \frac{A_D \, \Delta F^{1/2}}{D^*}$$

where A_D = 2 mm x 2 mm and ΔF is a function of the integration time selected on the lock-in amplifier and the frequency of the signal. The noise voltage (and hence D*) as a function of frequency for the detector-preamplifier combination is shown in Figure 3-12. The NEP for the detector element parameter with the exception that ΔF (a system related parameter) is included.

A more useful parameter that describes the radiometric performance of the entire optical system is the Noise Equivalent Radiance (NER). It is defined as the change in radiance at the source that produces a signal equal to 1 RMS noise voltage at the sensor output.

3.6.2 System Tests

A photograph of the optical system is shown in Figure 3-13; Figure 3-14 is taken at a different angle so that the majority of the supporting systems can be seen. The following tests were made with the various components in this configuration.

Noise Equivalent Radiance

The NER was defined in 3.6.1 above; in its definition it is assumed that the radiance from the source fills the field of view of the optical system.

Both the sample cell and PM cell were evacuated, the black body was set at a temperature T_B°K. The Brower chopper was set to rotate at the PM frequency and

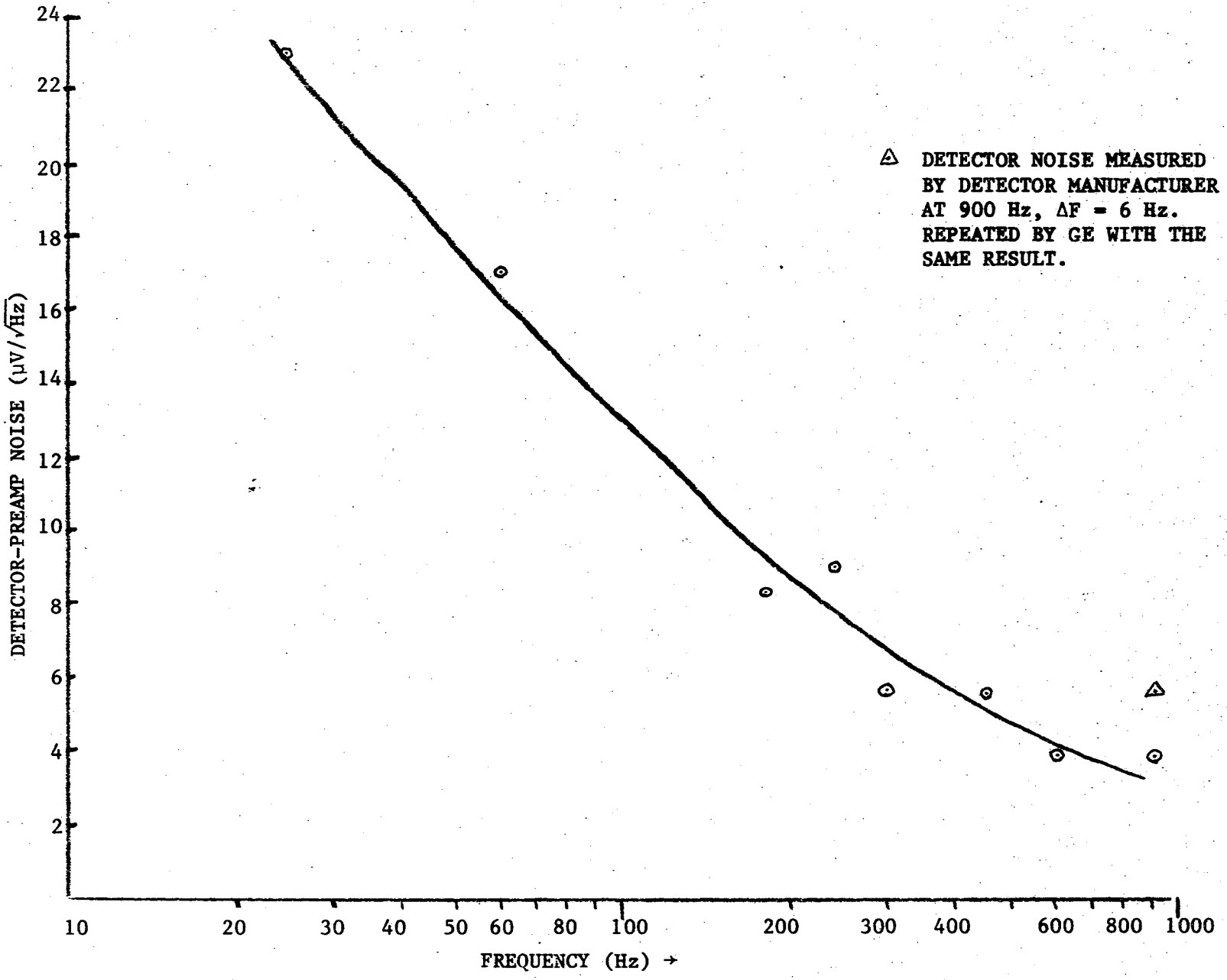

Figure 3-12. Detector-Preamp Noise Vs Frequency

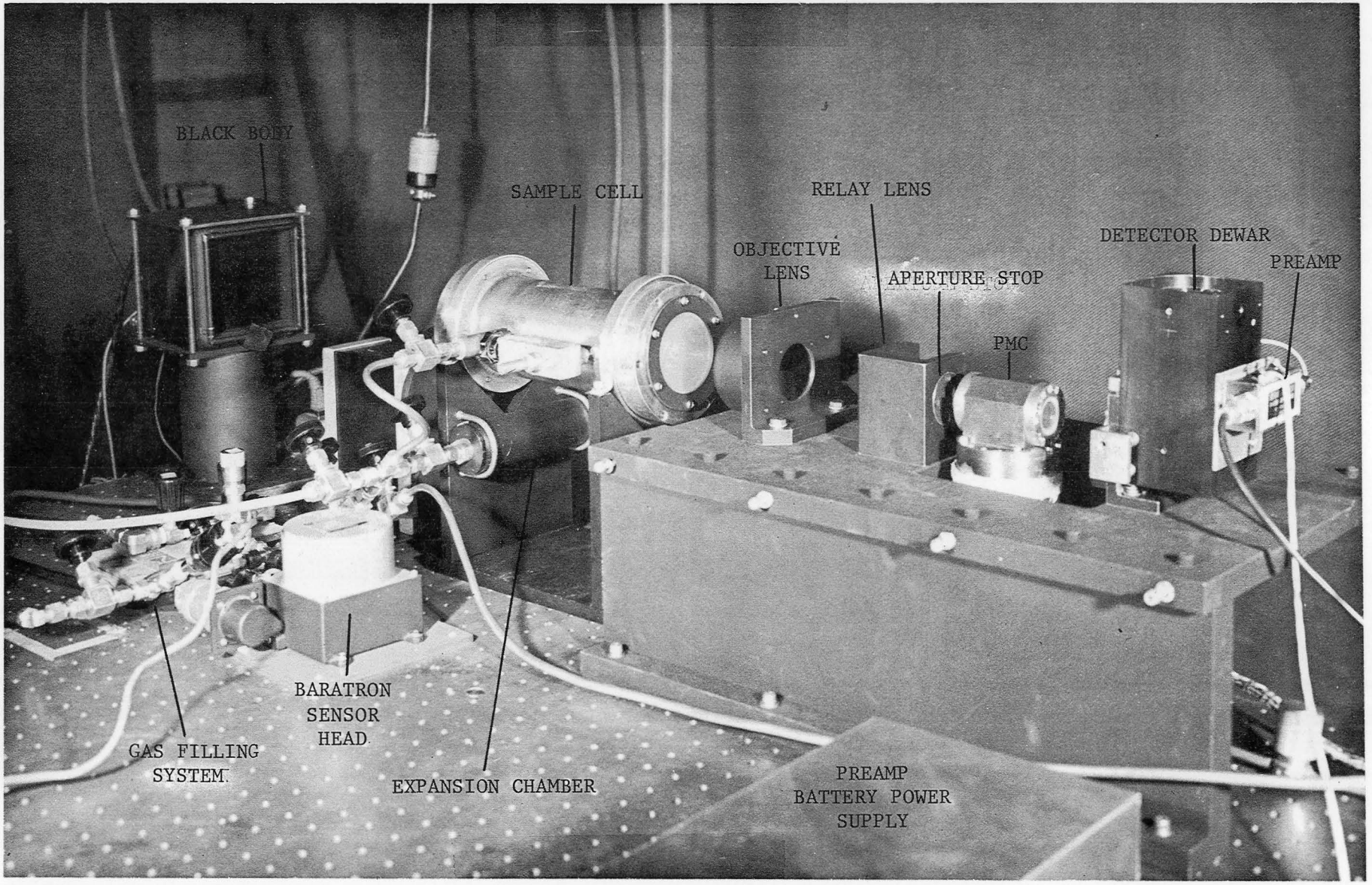

Figure 3-13. The Optical System

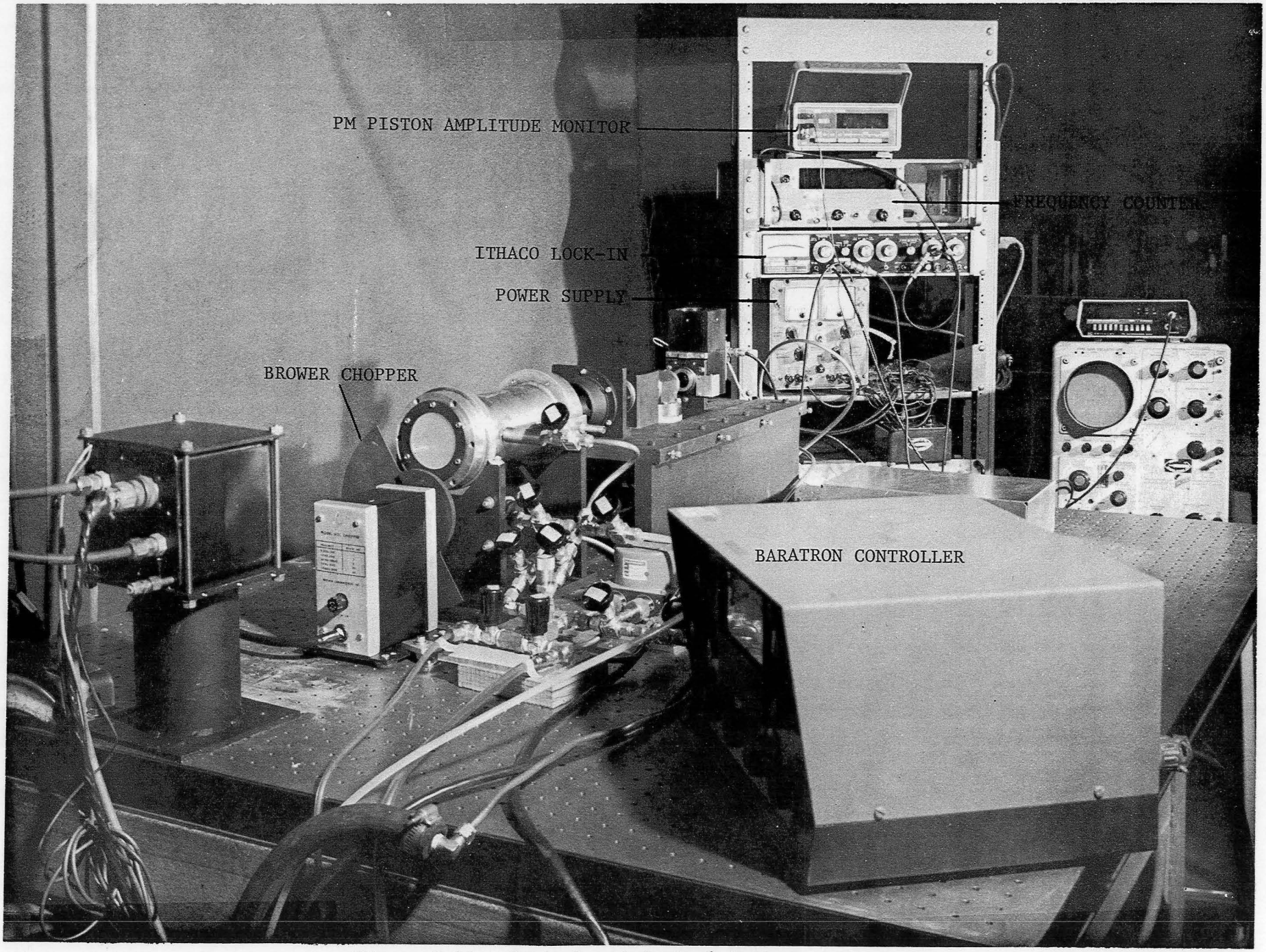

Figure 3-14. Optical and Control Systems

T_B adjusted so that a substantial signal was developed at the preamp output. T_B was then decreased in decrements and the signal output measured at each temperature setting. From the gradient of the curve of T_B vs. signal output, and the preamp noise at the PM frequency, the noise equivalent radiance was calculated.

The calculated procedure was as follows: the black body temperature was set at 5^oK intervals over the range 295^oK to 315^oK. At each setting the output voltage was measured. The in-band (4.46μ 4.85μ) fraction of this was calculated and the in-band radiance change that developed a signal change of 1 mv was determined. This was then used with the noise measurements made with the wave analyzer for the same frequency as that of the chopper. From the ratio of these two results the value of the NER was found to be 9.65×10^{-10} watts/cm^2/ster. Note that this applies to full bandwidth (4.46 - 4.85μ or 184 cm^{-1}) of the narrow band filter in front of the detector; it is NOT the NER for the 'chopped' bandwidth of the PMR which is of the order of 2 cm^{-1}.

This value applies when the source is a continuum (or planckian) radiator. The effective source in this experiment is a line radiator, for which the equivalent width of the emitting radiator is of the order of a few cm^{-1} as compared with 184 cm^{-1} in the measurement described above. The effective NER per cm^{-1} for line radiators for the optical system is therefore $184 \times 9.65 \times 10^{-10}$ watts/cm^2/ster or 1.77×10^{-7} watts/cm^2/ster (1 cm^{-1} bandwidth).

The most meaningful NER measurement for the PM sensor must be made with the PM cell active. The Brower chopper was therefore removed from the field of view; the PM drive was activated with a mean pressure of 8.5 mm of CO in the PM cell. As before the black body was set at selected intervals over about a 30^oK temperature range and the system output measured at each setting. A table was then generated in which the change in radiance was tabulated against the change in voltage Δv: this is shown in Table 3-4.

TABLE 3-4. INCREMENTAL SOURCE RADIANCE VS. PM SIGNAL OUTPUT

ΔR watts/cm^2/ster	ΔV volts
2.97×10^{-5}	0.2
2.89×10^{-5}	0.18
2.64×10^{-5}	0.15
2.037×10^{-5}	0.16
1.79×10^{-5}	0.12

The detector noise voltage at the system output was 0.010 volts. Therefore using this and the mean of $\Delta R/\Delta V$ from Table 3-4, the NER was found to be 1.49×10^{-6} watts/cm^2/ster per chopped bandwidth in cm^{-1}. The ratio of 1.77×10^{-7} w/cm^2/ster and 1.49×10^{-6} watts/cm^2/ster per chopper bandwidth is equal to 0.12 cm^{-1}. The reason for this small bandwidth (which should be about 10 times larger) is not known at this time.

This measurement concluded the system shakedown tests and the series of measurements to be made on CO and N_2O were begun.

4.0 TASK 4 - MEASUREMENTS OF GAS CONCENTRATION

4.1 INTRODUCTION

In this task the sample cell and expansion chamber were used to contain a mixture of carbon monoxide, nitrogen, and nitrous oxide gases. By systematic changes of pressure in the sample cell, it was possible to simulate the optical properties of the same species of gas in the atmosphere at many atmospheric levels. The experimental data was analyzed to show the sensitivity of the system to changes in concentration of the gases, gas mixtures, and to fluctuations in the background radiance.

4.2 BASIS OF THE EXPERIMENTAL PROCEDURES

The experimental procedure that was followed is based on theoretical and empirical relationships that have been found for the vibration rotation spectra of diatomic and polyatomic gases. Using these it was possible to control the gas parameters in the laboratory apparatus so that the radiant signal falling on the sensor was a good simulation of the signal the same sensor would receive from a satellite platform.

The fundamental property of the vibration rotation spectra that is used is that the equivalent width of a spectral line can be controlled through the total number of molecules and the mean pressure of a gas over a given path length. The fundamental relationship for the equivalent width is for strong, non overlapping lines:

$$W = 2\ \Sigma(S\ \alpha\ U)^{\frac{1}{2}}\ cm^{-1} \qquad (4\text{-}1)$$

where S is the line strength; α is the half width at half maximum; and U is the optical depth. For nadir paths through the atmosphere the optical path is non homogeneous; the Curtis-Godson approximation is then used and the expression for W becomes:

$$W_A = 2\left[S\ \alpha_o\ C_A\ H\ \frac{P_1^2 - P_2^2}{2}\right]^{\frac{1}{2}}\ cm^{-1} \qquad (4\text{-}2)$$

where C_A is the gas concentration in the atmosphere; H is the scale height; and P_1 and P_2 are different altitudes in the atmosphere. For the same gas in a gas cell in the laboratory of length Lcm and pressure P_2, the equivalent width is given by

$$W_L = 2\left[S\ \alpha_o\ C_L\ P_L^2\ L\right]^{\frac{1}{2}}\ cm^{-1} \qquad (4\text{-}3)$$

where C_L is the gas concentration in the laboratory cell. When $W_L = W_A$

$$\left[S\ \alpha_o\ C_L\ P_L^2\ L\right]^{\frac{1}{2}} = \left[S\ \alpha_o\ C_A\ H\left(\frac{P_1^2 - P_2^2}{2}\right)\right]^{\frac{1}{2}} \qquad (4\text{-}4)$$

and

$$\left[P_L\ \ C_L\ L\right]^{\frac{1}{2}} = \left[C_A\ H\left(\frac{P_1^2 - P_2^2}{2}\right)\right]^{\frac{1}{2}} \qquad (4\text{-}5)$$

Assuming C_A, H, C_L and L are constant

$$P_L = \text{Const}\left(\frac{P_1^2 - P_2^2}{2}\right)^{\frac{1}{2}} \qquad (4\text{-}6)$$

By changing P_L in the laboratory cell the optical depth of different path lengths in the atmosphere can be simulated. Using this approach the simulated atmosphere can be "sounded" by progressively decreasing the pressure in the cell.

The final parameter that is controlled is the mean pressure of the PM cell. During pressure modulation the profiles of the spectral lines of gas contained in the cell change their equivalent widths about a mean value. The mean value is determined by the mean pressure in the PM cell; by appropriately selecting the mean pressure the PM sensor can be made sensitive to a particular altitude range.

The optical properties of a gas in the atmosphere vary with altitude, the

incremental transmission per unit interval of optical depth is called the weighting function. For uniformly mixed gases monitored by a PMR, the weighting function is related to the mean pressure of the gas in the PM cell by the expression

$$P_{Pk} = \left[\frac{4\ (1 + \alpha_b)}{a} L \right]^{\frac{1}{2}} \overline{P}_C^* \qquad (4\text{-}7)$$

where P_{Pk} is the atmospheric pressure of the peak of the weighting function; α_b is a broadening coefficient of the gas; a is the atmospheric burden of the gas; and $\overline{P}_C$ is the mean pressure of the gas in the PMC.

The results expected from an experiment with the following parameters were calculated for the CO-P_4 line: L_{cell} = 20.32 cms; $C_L = 8 \times 10^{-3}$; P_L initial 380 mm (Hg); $L_{PM\ cell}$ = 6 cms; C_{PMC} = 22 mm (Hg); P_{max}/P_{min} = 2:1; S_{P_4} = 6.5 cm^{-1}/atm cm; $\alpha_o = 0.05\ cm^{-1}$; $C_A = 1 \times 10^{-7}$; $H = 8 \times 10^5$ cms. The weighting function derived for the experiment simulation is shown in Figure 4-1.

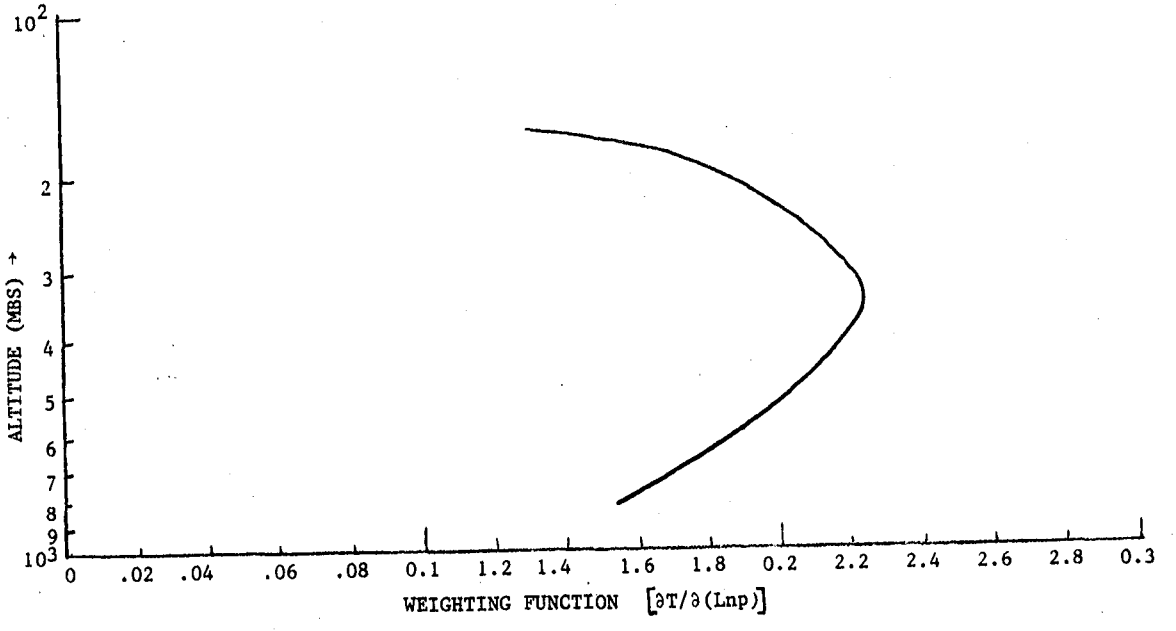

Figure 4-1. Calculated Weighting Function for 6 cm PM Cell at 22 mm Mean Pressure of CO

*"Radiometer for the Remote Sounding of the Upper Atmosphere", F.W. Taylor et al, Applied Optics, January 1972, Vol. II, No. 1, pp 135-141.

The experimental results will be slightly different from those calculated for a single line because the passband of the filter includes at least fifty lines of differing strengths and widths.

4.3 EXPERIMENTAL RESULTS

The prime objectives of the experimental program were to establish

(a) The sensitivity of the PM sensor to changes of concentration of CO in the atmosphere.

(b) Determine the effect (if any) of a random fluctuating background on the CO concentration measurement.

(c) Show that N_2O can be used to measure the in-situ temperature of CO in the atmosphere.

Preliminary measurements were made with the experimental apparatus to experimentally verify the theoretical predictions in paragraph 4.2. The experimental parameters were the following:

Run 1

PM Cell - length 6 cm; Mean Pressure - 11.6 mm; Pure CO (C = 1); Sample Cell - length 20.32 cm; Initial Pressure - 380 mm total; CO concentration - 8×10^{-3}; Diluent Gas N_2; Black Body Temperature $\approx 75^{\circ}C$; Sample Cell and PM Cell at room temperature $\sim 25.6^{\circ}C$.

Run 2

All the above parameters the same with the exception of the CO concentration which was increased to 9.6×10^{-3}.

The first experiment simulated an atmospheric CO concentration of 100 ppb and the second a CO concentration of 120 ppb.

The experimental procedure consisted of filling the sample cell with CO and N_2 at a total pressure of 380 mm; the detector output was then measured.

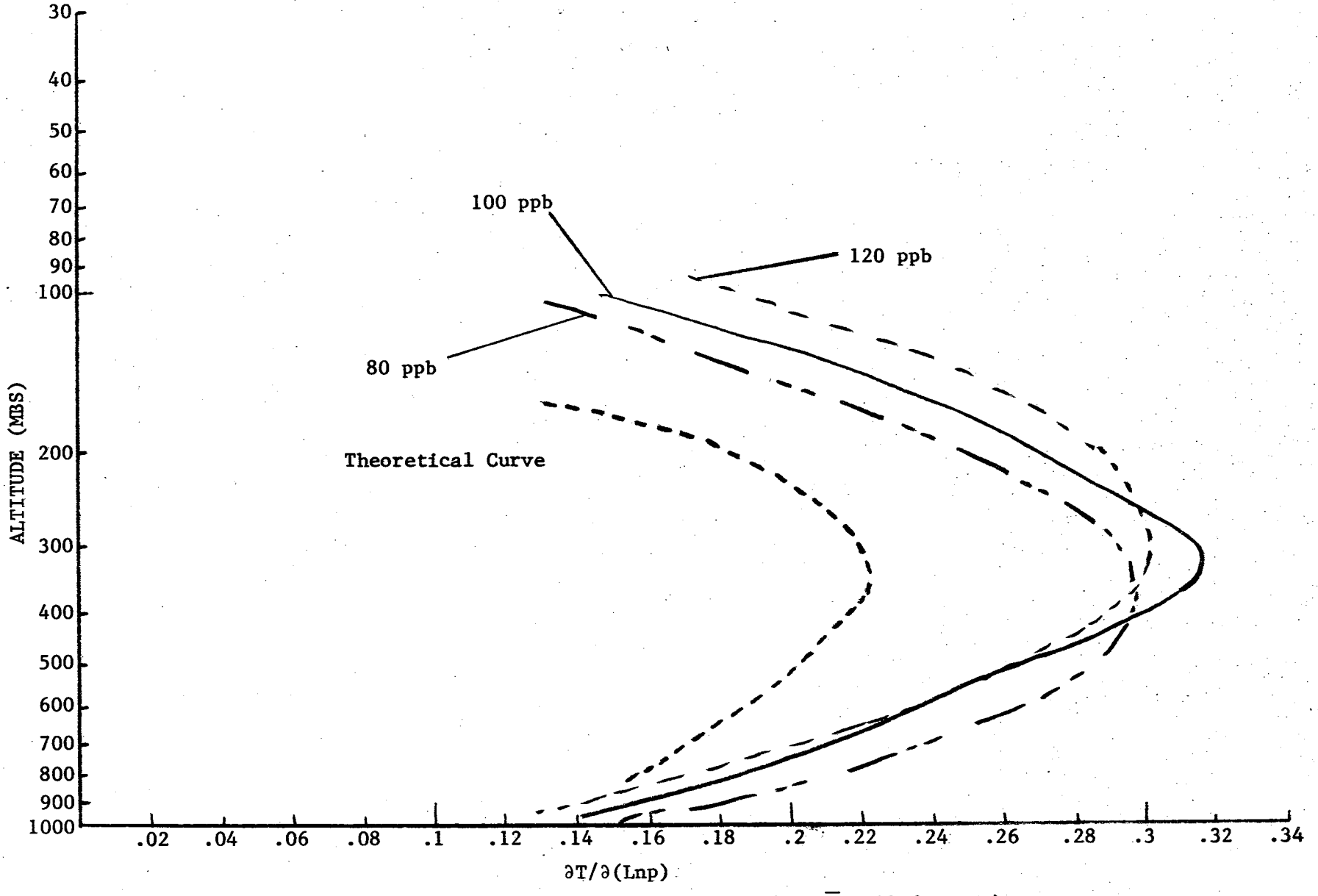

Figure 4-2. Weighting Functions for Pure CO (PMC $\overline{P}$ = 11.6 mm Hg)

The total pressure in the sample cell was decreased by 15% and the detector output again measured. This procedure was repeated twenty times; finally the sample cell was evacuated and the detector signal measured.

The weighting function was derived by determining the incremental transmission of the gas in the sample cell and plotting this against the equivalent (mean) altitude of the atmosphere at each step. The results of these preliminary experiments are shown in Figure 4-2 with the theoretical prediction of the experiment (at a higher PM cell pressure) shown for comparison.

The spread of the experimental points were due to a steadily increasing PM signal output. This was caused by a gradually increasing mean pressure in the PM cell. These results show that an increase of CO concentration causes the effective peak of the weighting function to occur at a higher altitude. When this occurs in the atmosphere there is (an accompanying) change in the mean radiance of the gas due to the lower temperature of the gas at the higher altitude (troposphere); this was not simulated in the experiment. This demonstrates why it is important to have a direct measurement of the temperature profile of the gas when a measurement of concentration from a satellite is made.

These experiments were made at a higher background radiance than was originally intended. This was due to the large offset signal caused by the (apparent) adiabatic heating of the gas in the PM cell during the pressure cycle. This offset signal increased with increasing pressure in the PM cell.

Steps were then taken to eliminate the cause of the pressure increase in the gas cell. The PM cell had been helium leak tested prior to the experimental measurements, but no leaks were found. A prolonged pumpout of the PM cell at an elevated temperature did not eliminate the pressure rise which had been attributed to an internal component outgassing. Further leak tests were made using helium bags around the PM cell; initially these were negative. Eventually

it was found that the helium required at least 15 minutes to diffuse through the leaking area. This was an epoxy seal that was partially closed off from the atmosphere by the window mount; the epoxy seal was drilled out and replaced with new epoxy.

The system was again leak tested but a very small leak still persisted which could only be detected by surrounding the PMC with a polyethylene bag filled with helium. The leak testing procedures indicated that the leak was not confined to a localized area, like a pinhole. An investigation of the elastomers used for "O" rings revealed that they were permeable to the gases in the atmosphere. Rough calculations indicated that the four 1" diameter seals and the one 2" diameter seal would leak into the cell an amount of gas that would raise its pressure by about 50 microns in a 24-hour period. This is somewhat less than the 100 to 200 micron increase that is observed over a 24-hour period.

The modifications needed to seal the cell and window were completely out of scope with respect to the funds remaining in the program and the time available. Measurements were continued with the leak still present. The behavior of the cell pressure was subsequently found to be somewhat erratic; very stable over some periods and erratic in others. In general the mid-day behavior was erratic (possibly associated with the laboratory temperature). The requisite number of runs to complete the task were made; but were at times significantly affected by the instability of the IR signal caused by the signal drift. The weighting function measurements were the most severely affected, because the signal outputs between consecutive measurements had to be taken in order to determine the incremental transmission.

These results are shown plotted in Figure 4-2; note that the peak of the weighting function moves to a higher altitude as C, and hence "a", increases in accordance with the expression given in Section 4.2. The percentage increase in

altitude caused by the 20 percent increase in C is also in agreement with this equation.

The shape of the weighting function curve is not as sharp as it would be if a very narrow band filter had been used. However the altitude selectivity shown in the curves is quite satisfactory.

4.4 CONCLUSIONS

The experimental results are in good agreement with the theoretical predictions and convincingly validate the laboratory simulation approach. The accuracy of the experiments were impaired by the leaking "O" rings but modifications to the cell could overcome this difficulty.

5.0 PM SIGNAL SENSITIVITY TO A TIME VARYING BACKGROUND

5.1 INTRODUCTION

The objective of this experiment is to examine the effect (if any) of a time varying radiance on the PM signal. In the laboratory simulation the time varying radiance is generated by a thin hot wire, through which an alternating current is passed.* The hot wire is stretched across a black body which provides the background radiation that simulated the steady component of the earth's radiance.

The electronic apparatus needed to generate the alternating current for the wire is shown in Figure 5-1. The prescribed procedure for this system was to operate the wire at a steady temperature of $1200^{o}K$. The AC current was adjusted to produce a temperature change of $\pm 20^{o}K$ at frequencies varying from 1 Hz to 50 Hz.

As a result of an unexpected feature of the pressure modulator signal output, this procedure could not be used to provide the intended 3-5% time varying modulation of the PM signal. The technique adopted and the signal characteristics that were found are described in the following section.

5.2 EXPERIMENTAL PROCEDURE

The original test plan was to control the alternating radiance from the hot wire so that it developed a signal at the detector output whose RMS amplitude was between 3% and 5% of the pressure modulator output. The latter signal was about 500 microvolts, therefore the alternating component should be between 15 and 25 microvolts.

Inspection of Figure 3-12 showed that at this amplitude the A/C component would be equal to or less than the detector noise. The measurement of the latter was repeated and is shown in the lower part of Figure 5-2. Note that the shape of the curve differs from that obtained earlier and also the amplitudes at each frequency were significantly less.

---

*This instrument was designed and built at La.R.C.

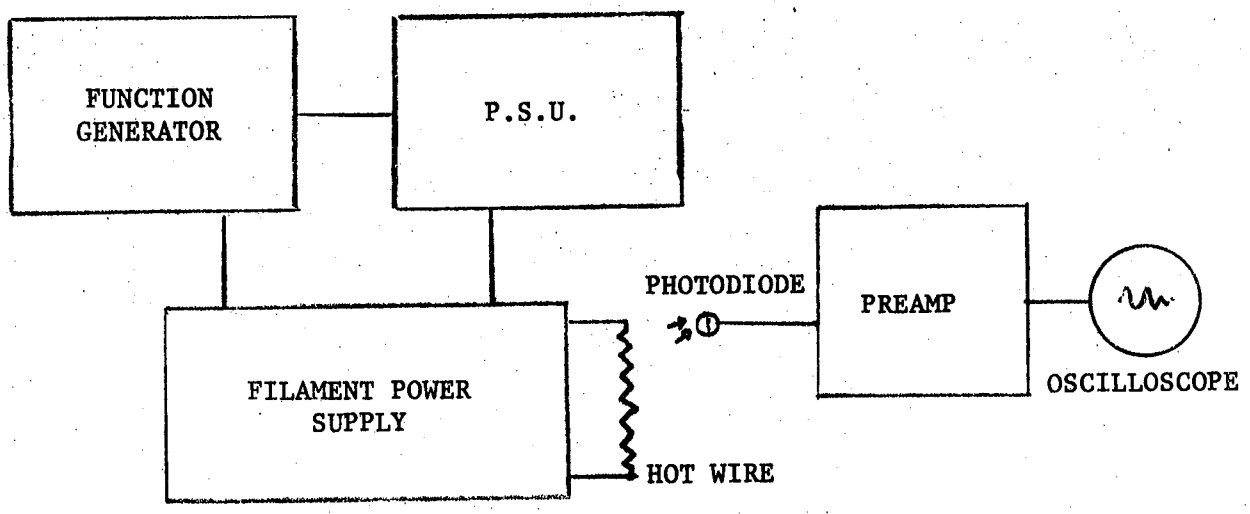

Figure 5-1. Block Diagram of Hot Wire Control Circuits

During the first run with the PM cell operating it became evident that the S/N ratio for the A/C component was not as large as it had been calculated to be and so a further noise vs. frequency curve was measured with the PM cell operating. The results obtained at two different background temperatures are shown in the upper curves of Figure 5-2. They show that the probable noise at the PM frequency is about 15 μv or about 7 times greater than the PM drive is quiescent.

The reason for the decrease in detector noise over several months is not known. One possible cause discussed with the detector manufacturer was that the detector because it was mounted behind the narrow band filter, was not exposed to visible or near UV radiation. (These wavelengths are known to create traps in some IR detector materials.) It is interesting to note that the excess noise at the PM frequency could explain the apparent very narrow chopped bandwidth of the PMR.

5.3 DISCUSSION OF THE RESULTS

The noise vs. frequency curves in Figure 5-2 show that excess noise is generated by the action of pressure modulation. It is suggested that the effect is similar to that produced by swirling convection currents that surround the hot filament of an electric light bulb; these also produce excess noise. Adiabatic heating (and cooling) of the gas in the PM cell may result in a spatially varying temperature distribution of the swirling gas. This phenomenon could well give rise to the effect observed.

The unexpected characteristic of the noise vs. frequency distribution is that very low frequency noise is also generated. Swirling motion would be more likely to generate noise at frequencies that are higher than that of pressure modulation. The reason for this inconsistency is not known.

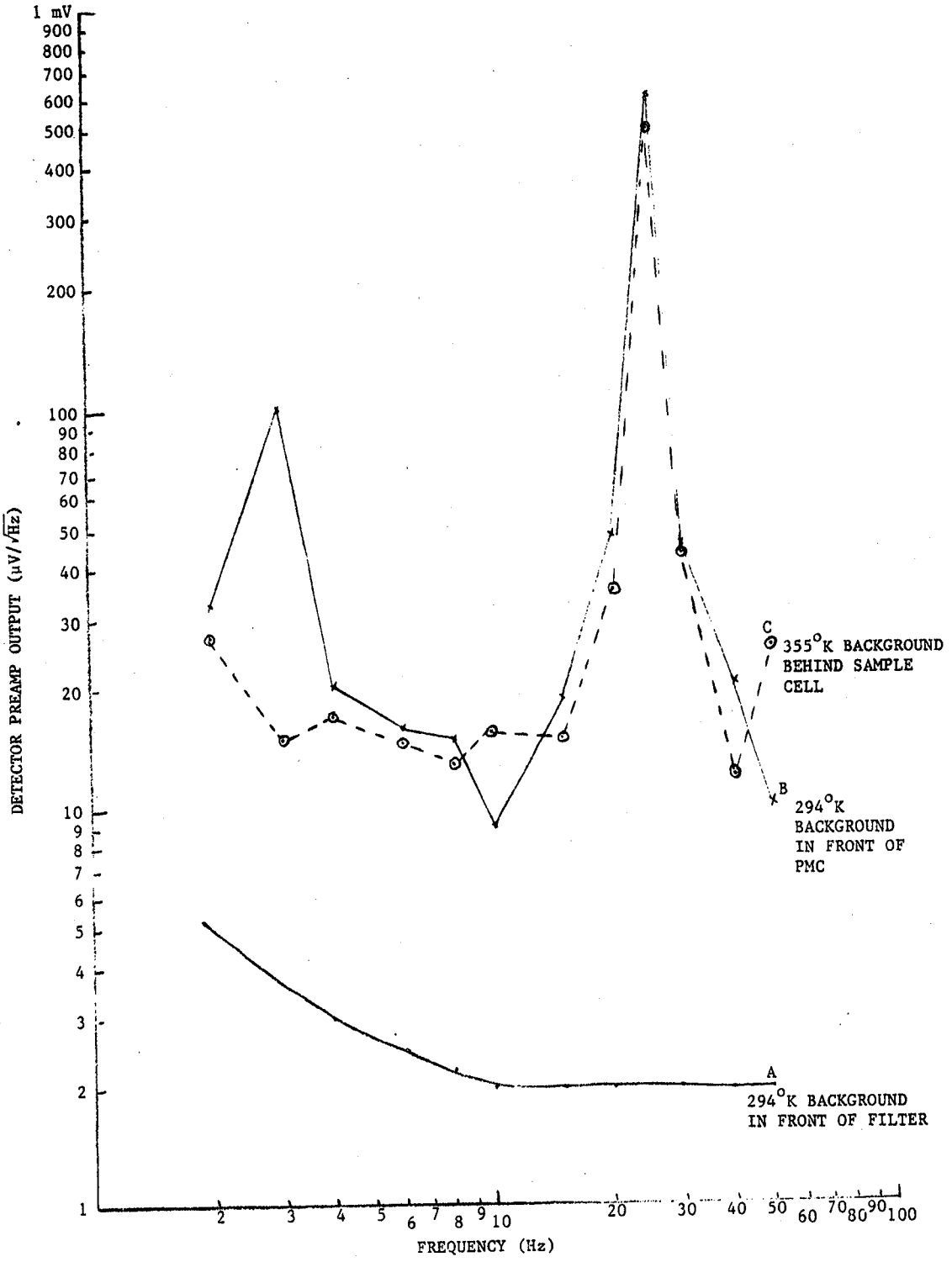

Figure 5-2. PMR Noise Voltage as a Function of Background Source Location

TABLE 5-1. INFLUENCE OF TIME VARYING RADIANCES

	AC RADIANCE FREQUENCY Hz	SIGNAL OUTPUT DURING AC RADIANCE VOLTS (LOCK IN OUTPUT)	SIGNAL OUTPUT WITHOUT AC RADIANCE VOLTS (LOCK IN OUTPUT)
	2	5.135	5.138
	3	5.154	5.150
	4	5.155	5.164
	6	5.166	5.171
	8	5.174	5.179
	10	5.186	5.189
	15	5.200	5.204
	20	5.233	5.236
	21	5.235	5.240
	22	5.401	5.406
	23	5.416	5.420
	24	5.428	5.433
	25	5.437-5.443	5.438
PM FREQ 25.8-0.9 →	26	5.424-5.485	5.449
	27	5.412-5.494	5.455
	28	5.455	5.453
	29	5.450	5.450
	30	5.451	5.450
	35	5.445	5.445
	40	5.443	5.445
	45	5.446	5.445
	50	5.446	5.446

NOTE: 1 sigma RMS noise ≡ ±0.008 volts

The other issue is the sensitivity of the PMC output to a time varying radiance. To simulate the time varying component of the earth's upwelling radiance, the source generator must be capable of providing random phase and amplitude at all frequencies. The source generator used in this experiment was set at a constant amplitude and a fixed frequency. However, the phase of this

signal could change relative to that of the PMC. Unpublished field data obtained near NASA Langley indicates that at 25 Hz the ratio of the amplitudes of the background AC to DC component is less than 1 in 10^3.

The affect on the output was measured to be less than 1½%; it is anticipated that this is an upper figure because background modulation will be varying in amplitude. Based on this result, the naturally occurring background modulation is expected to affect a PMC output signal considerably less than an amount of 1%.

6.0 OUTPUT SENSITIVITY TO N_2O INTERFERENCE

6.1 INTRODUCTION

The objective of this experiment was to determine the extent of the change of the PM output signal caused by CO lines overlapping those of N_2O. In those spectral regions where the tails of the spectral lines of the two species overlap, the modulated CO lines will generate signals (from N_2O) that are indistinguishable from those of CO lines. The magnitude of the signal change is dependent on several parameters, of which the filter bandpass, the PMC mean pressure and compression ratio are three of the more important.

6.2 EXPERIMENTAL PROCEDURE

In this experiment the sample cell was pressurized to 380 mm total pressure; the partial pressure of CO was 3.04 mm and the diluent gas pure N_2. The PMC was filled with N_2O at mean pressures of 7.5 mm, 10 mm and 12.5 mm. These pressures were used because at this time it was not known what mean pressure of N_2O would be used in the PMC for a true measurement simulation.

The radiant background for the sample cell was the black body used on Task 4; its temperature was maintained at 72°C. The experiment consisted of measuring the transmission of the gases in the sample cell by ratioing the signal output obtained with gases in the sample cell to the signal obtained when the cell was evacuated. Transmissions for the cell (simulated atmosphere) were obtained for the three mean pressures in the PM cell.

The experiment was repeated with CO in the PM cell at the same mean pressures used for N_2O. Finally to check out the system, the PM cell was filled with N_2 only, and as expected no PM signals were generated. The results of this experiment are shown in Figure 6-1.

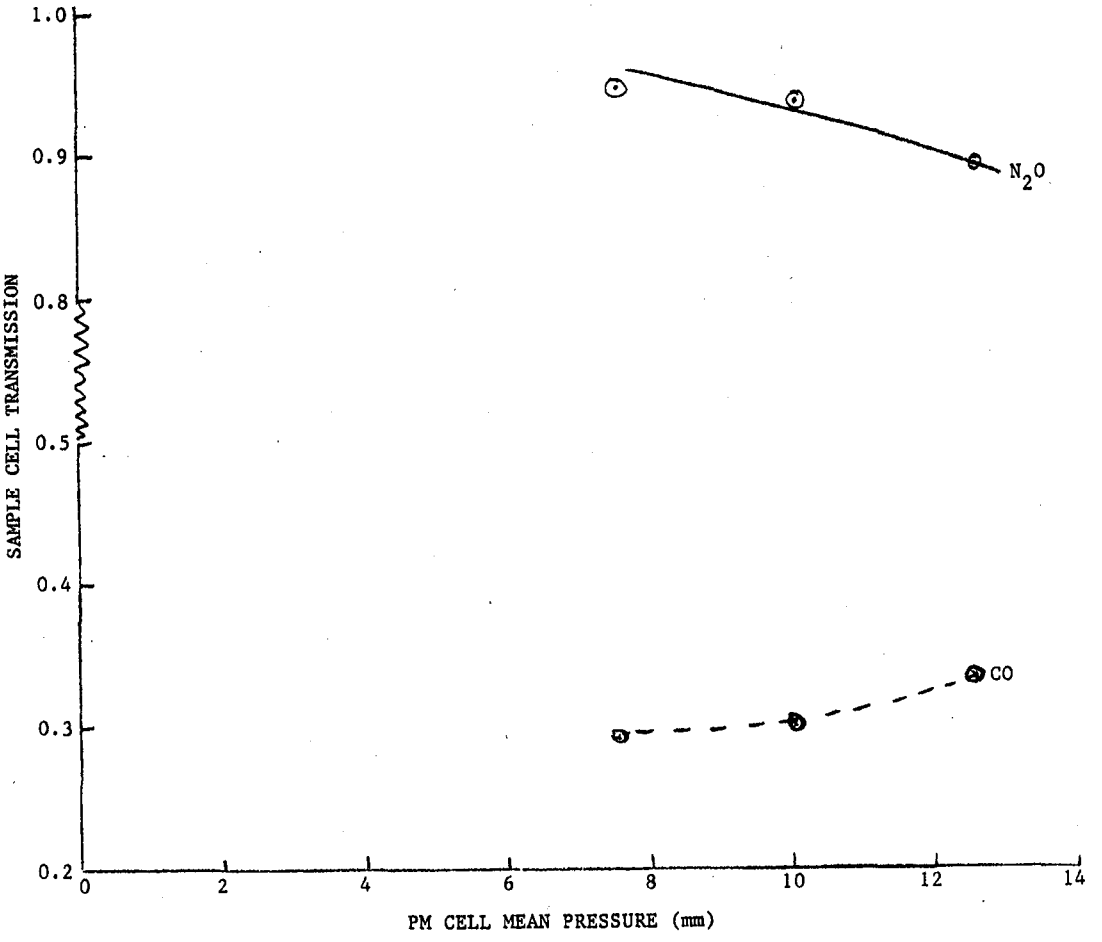

Figure 6-1. Sample Cell Transmission for Pressure Modulated N_2O and CO

6.3 DISCUSSION OF THE RESULTS

The first comment to make is that this important experiment should be carried out at greater depth than was possible in this program. For example, mixtures of CO, N_2O, N_2 and O_2 should be used in the sample cell to simulate the atmosphere more completely. Further tests should also be made with custom designed optical filters that isolate a specific part of the N_2O spectrum.

These preliminary results are quite informative however; the upper curve for N_2O in the PM cell indicates that the interference of N_2O will increase with the mean pressure used in the PM cell. This is expected because the width of the N_2O lines increase as the cell pressure increases and therefore more overlapping of the CO and N_2O lines occur. The modulated (N_2O) signal is diminished and hence the effective transmission also decreases. This implies that at high PM cell mean pressures, the interaction will be even greater than that indicated. This is not necessarily true for two reasons; the pressure required in the PM cell is a function of the strength of the part of the N_2O band used and the transmission of the narrow band filter over that range of wavelengths.

During the experiments the N_2O PM signal was about three times greater than that developed by CO at the same pressure. This was not expected and should be investigated further; however if it is correct the implication is clear, N_2O can be used at lower pressures or attenuated by the optical filter. Until the weighting function for N_2O is measured with this and other filters, it is not clear which approach can be used. It is possible, however, that the N_2O transmissions obtained in this experiment could be significantly higher than necessary.

The CO curve is reasonably straightforward to interpret. As the PM cell mean pressure increases the "chopped" part of each spectral line moves further from the line center (of the CO lines in the sample cell). Toward the wings of the lines the transmission approaches one, hence as the chopped region moves away from the line centers the gas transmission increases.

7.0 CONCLUSIONS AND RECOMMENDATIONS

7.1 CONCLUSIONS

7.1.1 Experimental Equipment

The arrangement of the sample cell and expansion chamber was effective in simulating the optical properties of CO in the atmosphere. For other trace gases at low concentration levels this arrangement is adequate. For more concentrated species such as $C^{13}O_2$ the apparatus should be in a vacuum environment or nitrogen tent.

The modified MAPS optical system was ideally suited for one or two PM systems. The optical train would have been easier to align if Irtran II had been used in place of germanium, however since the alignment was a one time only activity this is not a crucial issue.

A considerable amount of care has to be taken to ensure that the PMC can be effectively pumped out (without backup) by a dedicated pumping system. The access part of the PMC has a small diameter and should present the greatest impedance to the pumping system. It is particularly important to have a high pumping speed at this part and supported by a pressure sensor located in the optical head. This requirement is of some importance in laboratory apparatus because frequent changes in the PMC gas may be required.

7.1.2 Weighting Function Measurements

Although adversely affected by the PM signal drift caused by atmospheric gas diffusing through the "O" ring seals, the weighting function measurements showed clearly the altitude discrimination properties of the PM approach. The altitude separation of the curves and their relative positions were also sensitive to external gas diffusing the system. The required concentration and mean pressure of the gas in the cell were not always the same throughout the

time taken to complete the measurement. Further experiments should be performed to determine the pressure of N_2O in the PM cell that matches the weighting function of the CO while producing minimum interference.

7.1.3 The Effect of Background Modulation

The laboratory experiment showed that the PMR output is relatively insensitive to background radiance modulation. The test conditions represented what is thought to be a worst case situation in which the amplitude modulation was held constant at 20% of the PM signal (100μv in 500μv) and in which the phase of this modulation maintained a constant relationship with that of the PM signal.

The magnitude and phase properties of the upwelling radiance observed by satellite instrumentation is not known. Experiments conducted from a low flying aircraft by La R.C. personnel showed that the percentage modulation at typical PM frequencies is less than 0.1%; the phase variations were not measured. The area of the earth's surface scanned by the instrument on the aircraft at its operating altitude was significantly less than that for a satellite instrument.

Further useful experiments could be made in the laboratory using a hot wire source driven by a noise generator instead of a signal generator. These experiments would enable critical thresholds to be determined for the PMR approach.

7.1.4 N_2O Interference

The measurements made were not extensive enough to draw in depth conclusions about the degree of interference that would be caused by N_2O. There was obviously some interference, though as pointed out in Section 6, it may be possible by appropriately selecting the narrow band filter cut off and slope, to minimize the interference significantly. It is possible that through the relative concentration of CO and N_2O in the atmosphere and the selected altitude for the weighting function a certain level of interference will have to be accepted. More detailed

experiments supported by computer calculations are needed to clarify this issue.

7.2 RECOMMENDATIONS

Future work on the pressure modulator concept should be made with a PM cell that has good metal seals between the modulator section and the optical head. Metal seals could also be used for the windows but an epoxy seal is more attractive and durable. Care must be taken to ensure the epoxy used will not eventually break down chemically or react with the gases used in the optical head.

For laboratory measurements a fully instrumented optical head is recommended, in particular it should have the capability to measure the gas pressure and temperature in real time during the modulation process. This requires that the response time of the sensors should be less than 5 milliseconds.

It is also important to arrange for a dedicated vacuum system for the pressure modulator cell. Because the outlet valve of the cell will have in general a small orifice, the connecting tubing to the vacuum system must have an internal diameter of at least ½". A desirable but not essential piece of instrumentation that could be used on the vacuum pump-PM interface is a small quadrapole mass spectrometer. This would be extremely useful in evaluating the source of vacuum leaks and the products of any chemical reactions that may occur inside the PM cell.

Finally the measurements should be made with the sample gas containing appropriate mixtures of N_2O, CO, N_2 and possibly CO_2 and O_2 in the sample cell. The spectral characteristics of CO and N_2O may well be influenced by these gases in the atmosphere, and although it may always be possible to correctly simulate their partial pressures there in the atmosphere, the trend of possible interactions may be observed.

Finally it is recommended that future work should include an evaluation of the tandem operation of two cells whose oscillating frequencies are amplitude modulated on a wide band chopper signal and whose oscillating frequencies are within 1-2 Hz of one another. Tandem operation of two PM cells is highly desirable from several technical aspects but the adequate isolation of the signal content at each frequency must be experimentally demonstrated.